LAPPEENRANTA UNIVERSITY OF TECHNOLOGY

FACULTY OF TECHNOLOGY

ENERGY TECHNOLOGY

MASTER'S THESIS

WIND TURBINE OPERATION IN COLD CLIMATE

Supervisors and examiners: Professor, D.Sc. (Tech.) Dr. Jari Backman

M.Sc. (Tech.) Daniil Perfiliev

Lappeenranta, 2011

Svetlana Marmytova

Abstract

Lappeenranta University of Technology

Faculty of Technology

Degree Programme in Energy Technology

Svetlana Marmytova

Wind turbine operation in cold climate

Master's thesis

2011

64 pages, 44 figures, 4 tables and 2 appendixes

Examiner: Professor Jari Backman

                Master of Science Daniil Perfiliev

Keywords:

Wind blade, wind energy, ice accretion, aerodynamic parameters

The goal of the master's thesis is to determine and estimate ice accretion influence on the wind turbine blade performance. The thesis describes the technique of ice accretion calculation on the wind turbine blade and determination characteristics of the turbine with ice accreted. The methodology of the classic Blade Element Moment Theory was used. Iced blade experimental data was investigated in order to calculate blade with ice characteristics. The obtained results shows that iced blade power coefficient is lower than clean blade one. The heating system implementation shows that in the particular site in the Lapland region it is efficient.

ACKNOLEDGMENTS

This Master's Thesis was done in the Lappeenranta University of Technology.
I would like to express my gratitude to Professor Jary Backman and Master of Science Daniil Perfiliev for their assistence during this thesis carried out. In addition many thanks for their critical reviews and usefull advices.

Thanks to Professor Jary Backman as well as Lappeenranta University of Technology I had an opportunity to participate in the "WinterWind 2011" conference in Sweden. Information, that I've got during the conference helped a lot in my thesis development. I had an opportunity to talk with experienced engineers in my field of interests. The importance of such experience exchange hardly can be overestimated.

I would like to thank Project Coordinator Julia Vauterin for her support and desire to help during the whole education time in Lappeenranta University of Technology.
Special thanks I would like to say to my family for his supports through all my life.

Lappeenranta, May 2011
Svetlana Marmytova

TABLE OF CONTENTS

Abbreviations

LWC	Liquid water content
MVD	Median volume droplet
RMC	Rotating multi-cylinder device for measuring MVD and LWC
IRT	Icing Research Centre
LTHS	Large transport horizontal stabilizer
WECO	Wind Energy in COld climate
ADIS	Anti-icing and de-icing systems
BEMT	Blade element moment theory

List of symbols

a	Axial induction factor	
a'	Angular (tangential) induction factor	
a_n, a_{n+1}	Induction factors according to n and $n+1$ iterations	
B	Number of blades	(units)
c	Airfoil chord length	(m)
C_L	Lift coefficient	
C_D	Drag coefficient	
C_T	Thrust coefficient	
C_P	Power coefficient	
i	Angle of attack	
I	Turbulence intensity	
n_{rotor}	Rotor rotation frequency	(RPM)
N	Number of blade elements	
P	Output electrical power	(kW)
P_{rotor}	Rotor power	(kW)
P_{wind}	Input power of the wind flow	(kW)
Q_1	Tip losses correction factor	
Q_2	Hub losses coefficient	
Q	Resulted losses	
r	Radial direction	
R_{hub}	Hub radius	
R	Blade tip radius	
V	Wind speed on the hub height	(m/s)
β	Relative angle of attack	(deg)
γ	Twist angle	(deg)
λ	Tip speed ratio	
λ_r	Local tip speed ratio	
ρ	Air density	$(\frac{kg}{m^3})$
σ	Local solidity	
Ω	Blade rotation speed	$(\frac{1}{sec})$
ε_a	Relative difference for axial factor	
$\varepsilon_{a'}$	Relative difference for angular factor	

6

1. Introduction

The goal of the Master's thesis is to find out the influence of the ice accretion on the wind turbine blade performance and to estimate produced energy losses because of ice accretion on the blades. Nowadays there are two main methods of energy losses estimation: field measurements and aerodynamic calculations. Field experiments demand observation time long enough to make necessary conclusions. Also wind turbine should be already installed. On the first project stages it is cheaper and easier to make aerodynamic calculations of the wind turbine under consideration. The thesis presents an example of such aerodynamic calculation and power coefficient estimation.

The calculation block includes iteration process of wind blade characteristics determination, clean and iced blades characteristics comparison, annual produced energy losses because of ice accretion on the blade.

The classical moment theory was used to determine power coefficients. Aerodynamic coefficients of the iced blade were investigated in Germany in the frame of tunnel experiments. The thesis does not take into account blade characteristics change when Reynolds number changes. The energy losses obviously could be more representative and reliable if field experiments results were known. Because of these data lack the list of ice accretion conditions were assumed and wind turbine performance in different modes were analyzed and compared.

2. Cold climate wind energy development

In order to obtain the European Union goals in renewable sources of energy share more wind sources should be used. For many northern regions all over the world the best location for the wind energy stations placement are along coastal areas or on the top of hills. Cold climate regions posses larger wind potential due to higher air density. These areas are exposed to the icing events during the winter time. Moreover even operation in some sought regions can face icing accretion problems. Majority of cold climate operated turbines are located in open or forested terrain with average wind speed up to 7 m/s and altitudes more than 71m. The total potential is 10 times more than easily acceptable offshore sites. (Beurskens J. 2011)

Among the cold climate wind energy growth general drivers the next can be mentioned:

1. National renewable energy targets
2. Lack of other energy or renewable energy sources
3. Growing importance of security of energy supply
4. Increasing volatility of fossil fuel prices
5. Overall awareness on environmental issues

Cold climate specific drivers:

1. Employment and local development
2. Improving cost competitiveness
3. Technology development
4. Growing cold climate experience
5. Higher cost of offshore wind
6. Possibility to large onshore projects

2.1 Current situation

On the base of International Energy Association Task 19 was performed in order to collect information in wind power project development, construction and usage at areas where low temperatures and atmospheric icing affect on operation of wind

turbines. Task 19 aim is to reduce risk connected with cold climate and hence the cost of wind electricity produced in cold climates. This work was organized in 2001 year. Among the participants such countries can be mentioned as: Finland, Norway, USA, Switzerland, Canada, Germany, Sweden, Austria. Reports, statistics, experience in wind turbine in cold climate operation can be found on the official website of the VTT. In the frame of this task the next wind energy in cold climate figure were obtained.
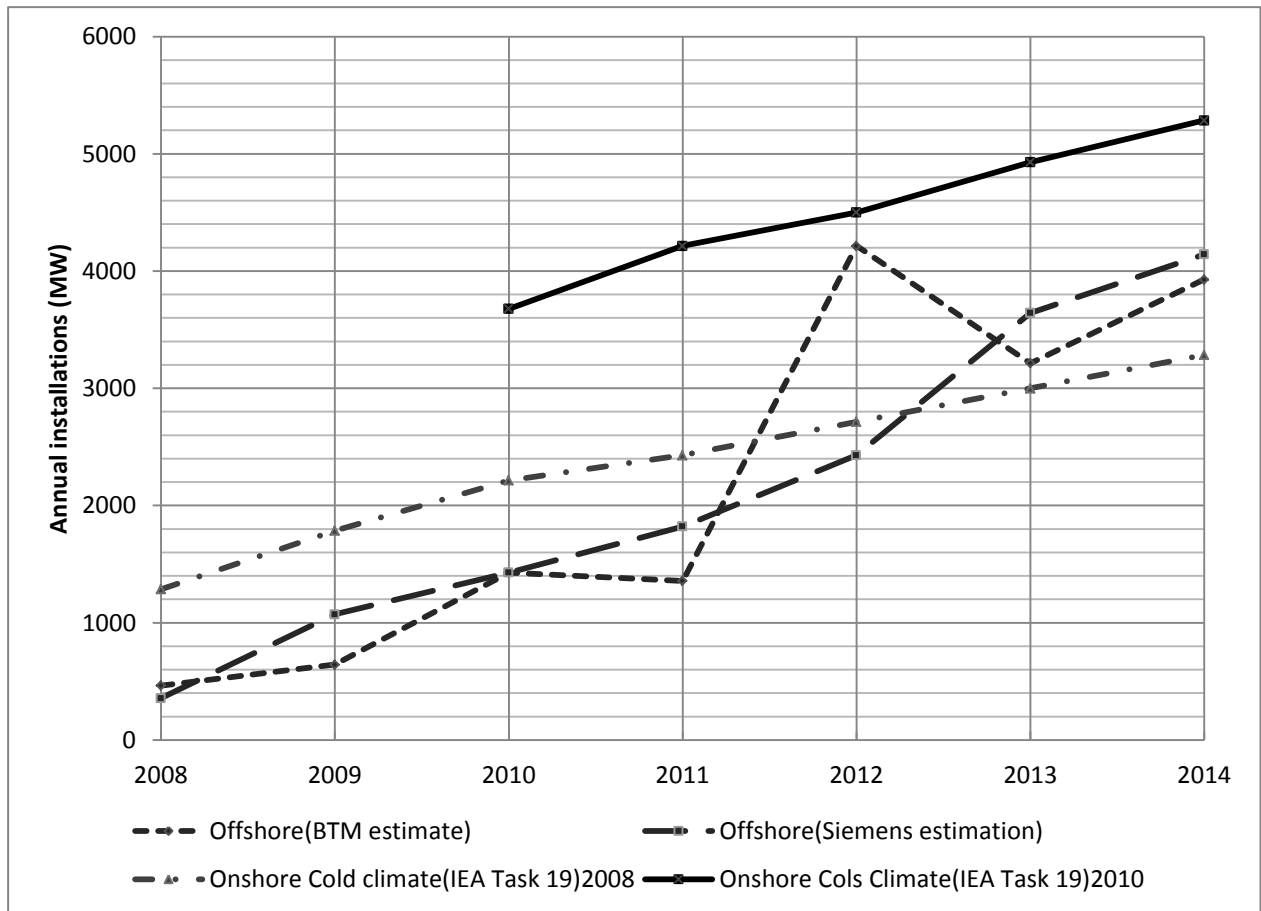

Figure 2.1.1 Estimated cold climate wind power market. (Laakso T., Tallhaug L. 2011)

Table 2.1.1 Some countries statistics. (Laakso T., Holttinen H. 2003)

	Scandinavia			Central Europe		North America
	Finland	Sweden	Norway	Switzerland	Germany	Canada
Cold climate capacity, MW	110/10	124(16%of total)	48,5	11,5/9,5	1000	1823/2239
Adapted cold climate technology, MW	50/5	13	1,5	1,5	-	1500/220
Cold climate potential, MW	3000/200[1]	30 000	2000[2]	3600	2500	45000/55000

[1]Technical and economical by 2020

[2]Notified or applied for to the Norwegian Water Resources and Energy Directorat (NVE)

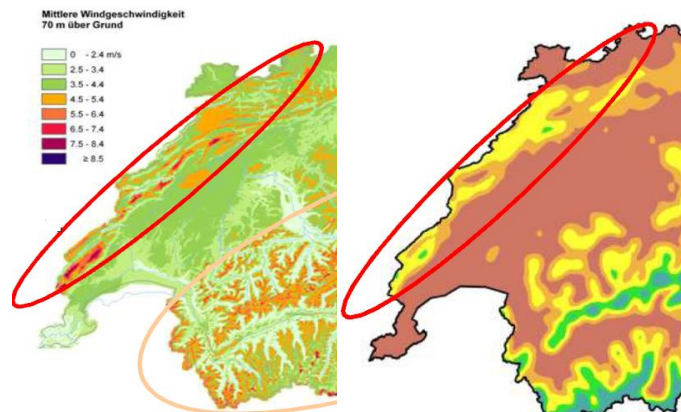According to Meteotest data almost all Swiss sites are considered to be in cold climate. (Cattin R. 2011)

Figure 2.1.2 Wind resources and cold climate conditions correlation in Switzerland.(Cattin R. 2011)

3. Ice accretion

For better understanding why icing occurs in some areas more often than others, and what causes wind turbines to be especially susceptible to icing, it is necessary to examine icing occurrence. In addition, several models for icing are presented.

3.1 Ice classification

There are two main types of atmospheric ice: in-cloud icing and precipitation. (Homola M. C., Nicklasson P. J., 2006) The main icing mechanisms of interest for wind turbine applications are as follows:

1) In-cloud icing

   a) Rime

Among the rime ice hard and soft rime, glaze can be mentioned.

2) Precipitation icing

   a) Wet snow

   b) Freezing rain

3) Frost

In-cloud icing occurs when small, supercooled, airborne water droplets freeze upon impacting a surface which allows formation of ice. These particles make up clouds and fog. These water droplets can remain liquid in the air at temperatures down to −35 °C

due to their small size, but will freeze upon striking a surface which provides a crystallization site. (Homola M. C., Nicklasson P. J., 2006)

The type of rime and glaze formation depends on the droplet sizes and the energy balance of the surface in question. In case of small droplets with almost instantaneous freezing, soft rime forms. With droplets of medium size and slightly slower freezing, hard rime forms. Rime appears white, and it can be broken easy than glaze.
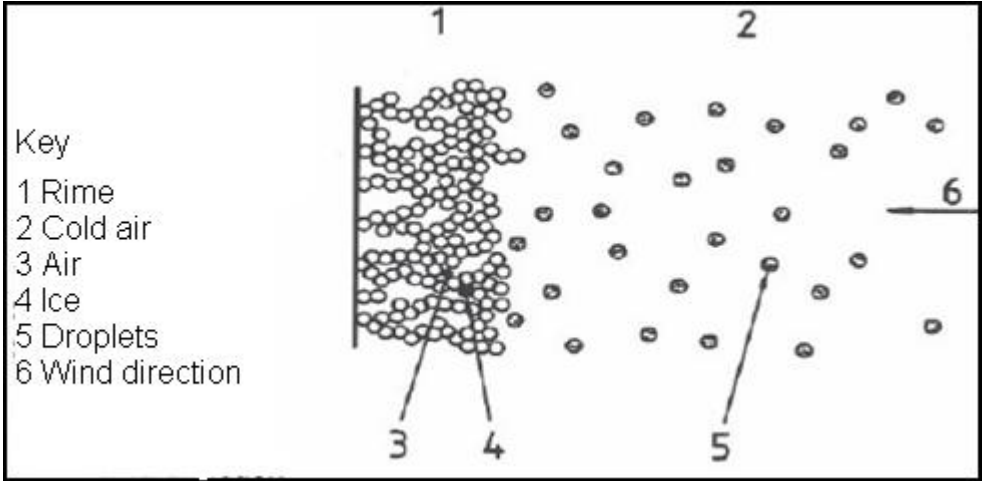

Figure 3.1.1 Growth of rime ice. (Homola M. C., 2005)

In case if the thermal energy released by the formation of ice from the droplets impacting the surface is not as quickly removed, and some portion of the droplets remains as liquid water the glaze is formed. Therefore there is always some liquid water present, and the surface temperature will be 0°C. Glaze appears as a solid covering of clear ice, because the low amount of trapped air. Glaze has a higher density compare to rime, and is more difficult to remove.
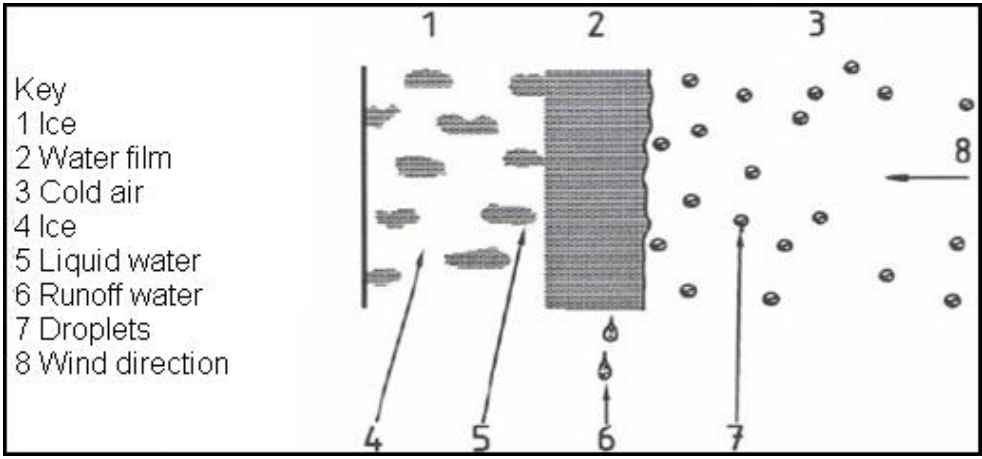

Figure 3.1.2 Growth of glaze ice. (Homola M. C., 2005)

Precipitation icing appears when rain or snow freezing is in contact with a surface. Precipitation icing can have much higher rates of mass accumulation than in-cloud icing, with possibly greater resulting damage. Relative frequency for the two types of icing is dependent on geographic location and climate.

Wet snow can stick to a surface in case if the temperature is between 0°C and 3°C. Since snow has some liquid water present, it allows the snow crystals to bind together when they come in contact on the surface. Wet snow often has a low binding strength while forming, but can become very hard and strongly bound if the temperature subsequently falls below 0°C.

When rain falls at temperatures below 0°C such appearing as glaze, freezing rain or drizzle can be observed. They often go along with the temperature inversion where cold air is trapped near the ground beneath a layer of warmer air. This can also occur in the case of a rapid temperature rise where an object still has a temperature below freezing nevertheless the air temperature is above freezing.

Frost is formed when the temperature of the surface is lower than the dew point of the air. Than water vapor to deposit on the surface forms small ice crystals.

3.2 Meteorological factors affecting icing

Table 3.2.1 contains some meteorological parameters that can be measured and have correlations with the type of observed ice.

Table 3.2.1 List of meteorological parameters affecting atmospheric ice accretion. (Homola M. C., 2005)

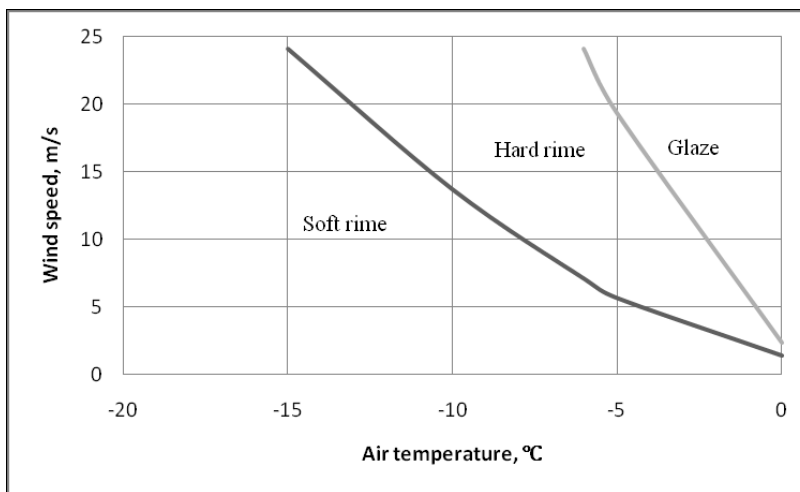| Type of ice	Air t° °C	Wind speed m/s	Droplet size	Water content in air	Storm duration
Precipitation icing					
Glaze (freezing rain or drizzle)	$-10<t_a<0$	any	large	medium	hours
Wet snow	$0<t_a<+3$	any	flakes	very high	hours
In-cloud icing					
Glaze	Figure 3.2.1	Figure 3.2.1	medium	high	hours
Hard rime	Figure 3.2.1	Figure 3.2.1	medium	medium	days
Soft rime	Figure 3.2.1	Figure 3.2.1	small	low	days

Figure 3.2.1 Types of accreted ice as function of air temperature and wind speed. (Homola M. C., 2005)

As a result of work, presented during the BOREAS VII conference, taken place in Finland in 2005, Makkonen has showed that among the temperature and wind speed the drop size distribution relative to the size of an object in danger of being iced-up and the liquid water content in air, are the primary parameters that influence the rate of icing. Although the relative humidity is the only parameter used to measure the icing accretion and appearance probability, as no other information exists. A major problem when comparing actual facts with the model simulations is that the drop size distribution and the liquid water content of air are, because of the lack of suitable sensors, not commonly measured. To determine the drop size distribution, Makkonen has suggested to use a multi-cylinder tube with seven cylinders of different sizes during measurements carrying out. The measured accumulated weight on every fourth among seven cylinder shows the average drop size distribution. Today, the prototype equipment is handled manually. According to Makkonen, visibility could be a suitable parameter to estimate the LWC of air. (Ronsten G. 2008)

3.3 Physical model of icing

A physical model of icing developed by Makkonen is described in the equation 3.3.1 (Makkonen L. (Ed.) 1994)

$$\frac{dM}{dt} = \alpha_1 \cdot \alpha_2 \cdot \alpha_3 \cdot w \cdot v \cdot A \qquad (3.3.1)$$

A —cross sectional area of the object with respect to the direction of the particle velocity vector,

w - mass concentration of the particles (rain drops, cloud droplets, snow or water vapor),

v - relative velocity of the particles,

The collection efficiency (or impingement efficiency), α_1, is the measure of the flux density of particles striking the surface in relation to the maximum possible. This coefficient usually is less than 1, because small particles are naturally follow the stream and are deflected from the surface striking.
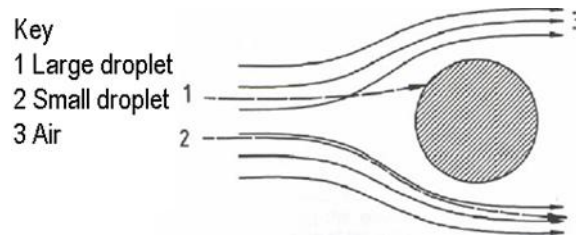

Figure 3.3.1 Droplet distribution according to its size. (Homola M. C. 2005)

Also it is important to mention that smaller objects are better collectors than larger one. Because with small objects the airflow in front of the object will have shorter radius flow lines when flowing around the object, which makes it more difficult for the water droplets to follow the airflow, due to their mass and velocity. Therefore more droplets will strike the surface than in the case of a larger object, where the droplets will be diverted from the surface by the flow of air. It means that even with the same conditions two different size objects can have entirely different rates of ice accretion.(Homola M. C. 2005)

The sticking efficiency, α_2, represents the ratio of the flux density of particles sticking to the surface to the flux density of the particles striking the surface.
The accretion efficiency, α_3, represents the rate at which ice builds up on the surface in relation to the flux density of particles sticking to the surface. This coefficient often is less than 1 because some of the particles, sticking the surface, become melted and running off. (Makkonen L. (Ed.) 1994) Presented models are strictly right and applicable to the cylindrical bodies. In case of wind blade some assumptions should be made.

Depending on the weather conditions different kinds of ice can be observed, but the temperature of the surface must be 0°C or below. The air temperature can be above 0°C if there is some combination of radiative and/or evaporative cooling, or in the case of a rapid increase in air temperature, such that the temperature of the surface is below 0°C. Relative humidity levels can be even lower than 90% to enable ice

accretion. Makkonen work shows that icing does not appear during periods of low relative humidity, and cast doubt over the accuracy of earlier humidity sensors for high relative humidity combined with temperatures below freezing. (Homola M. C. 2005)

3.4 Empirical model of icing

There are list of empirical model of ice accretion prediction with varying degrees of complexity. These models can be divided into two main classes: precipitation ice and in-cloud ice prediction.

As mentioned above existing models are developed for the cylindrical objects. The process scheme is presented in Figure 3.4.1 As an input parameters for the modeling one need to know at least the object radius R, the precipitation intensity I, and the wind speed V. More detailed and precise modeling requires the angle θ between the object axis and the wind direction, and the fall speed of the drops V_d, so that the drop impact velocity vector V can be determined. When V is known the flux density F=WV of the impinging water may be calculated in case if the liquid water content W in the air is known. The latter can be calculated from the equation 3.4.1.

$$W = \frac{\rho_w \cdot I}{V_d} \qquad\qquad (3.4.1)$$

ρ_w is the water density.

The drop fall velocity V can be determined from empirical expressions relating V_d , the drop size distribution and I.(Makkonen L. 1998)
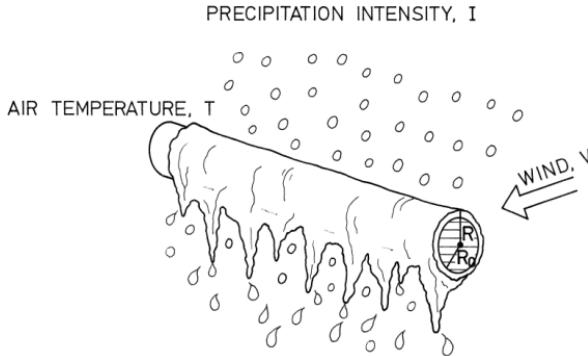

Figure 3.4.1 Icing in freezing rain. (Makkonen L. 1998)

Since the size of the drops is large the collision efficiency can be taken as 1. Nevertheless water collected by the object can be partly lost on shedding. Also runback water can form icicles. In its turn icicles form additional surface for ice

accretion. The basic challenge for the empiric models is clear understanding of the ice accretion process since almost necessary parameters can be obtained.

Imai model base idea supposes that heat transfer from the object influences on the icing intensity. So precipitation intensity I has no effect. It suggests that the glaze mass growth per length unit as described at equation 3.4.2

$$\frac{dM}{dt} = C_1 \cdot \sqrt{V \cdot R} \cdot (-T) \tag{3.4.2}$$

C_1 is a constant.

Equation 3.4.2 integration gives the result equation 3.4.3

$$R^{\frac{3}{2}} = C_2 \cdot \sqrt{V} \cdot (-T) \cdot t \tag{3.4.3}$$

Fixed ice density $(0{,}9 \ g/cm^{-3})$ is assumed and t is time.

However recent researches shows that heat transfer also affected by surface characteristics as roughness and evaporative cooling, also wet growth conditions not always prevail to -5 ºC, as assumed by Imai. That is why the presented model overestimates ice loads under typical conditions.

Goodwin model assumes that all collected drops get freeze on the object. The growth mode is dry. Then the accretion rate per length unit of the object as described in equation 3.4.4

$$\frac{dM}{dt} = 2 \cdot R \cdot W \cdot V_i \tag{3.4.4}$$

R is object radius,

W is liquid water content in air,

V_i is the drop impact speed. (Makkonen L. 1998)

To speak about the in-cloud ice prediction models formula found by Makkonen and Ahti should be mentioned. Nevertheless during the experience life it shows ice load overestimation and it was refined by Tammelin and Säntti (Makkonen L. 1998) into the form as described in equation 3.4.5

$$I = 4{,}8 \cdot 10^{-3} \cdot V \tag{3.4.5}$$

V is wind speed.

This formula application is feasibly if the conditions of being within a cloud and having a temperature below freezing are fulfilled. (Homola M.C. 2005)

3.5 Ice accretion mapping

It is not possible to describe typical cold climate condition, since with the different meteorological conditions ice can be accreted. For example in the areas with low average temperature ice accretion is not appeared, at the same time in the areas with mild temperatures heavy ice accretion is observed. Each site is different and requires more or less individual approach in ice-related measurements. In general as cold climate sites can be described those which have either icing events or lower than operational temperatures.

In Finland the average temperature is lower than the normal wind turbine operation one, however icing conditions can be observed only in Lapland region. High elevation, icing and -13 ºC monthly average temperature make conditions challenging.
As long as the cold climate areas become more attractive for wind energy sector it is necessary to obtain icing condition information in order to make equipment choosing process easy and reliable during project development.

Ice maps can be made on the base of meteorological data from weather stations. This source advantages are availability for a long period and relatively good spatial coverage. The disadvantage is that correlation between the predicted by meteorological data and icing conditions can be low. Meteorological data from airport weather stations can be used to predict ice accretion. Figure 3.5.1 shows ice frequency map in Europe, reported by Wind Energy production in Cold climate.

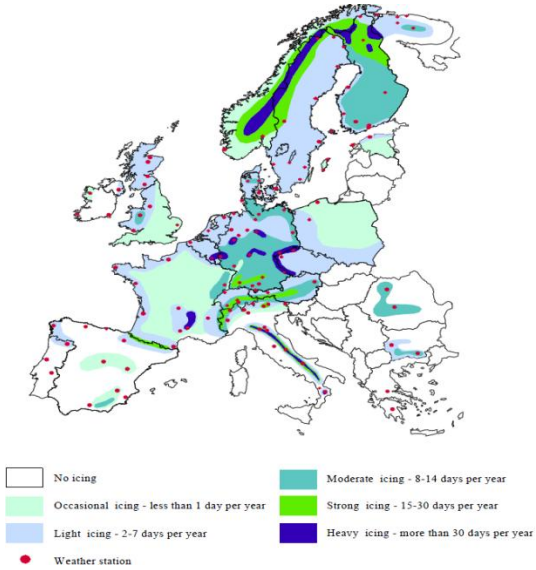|	
No icing	Moderate icing - 8-14 days per year
Occasional icing - less than 1 day per year	Strong icing - 15-30 days per year
Light icing - 2-7 days per year	Heavy icing - more than 30 days per year
• Weather station	

Figure 3.5.1 Icing days frequency. (Laakso T., Holttinen H. 2003)

Obtained results are based on the airport measurements with interpolation between the weather stations. Presented map does not take into account local topography.

A more precise ice British Isles map with the topography consideration is presented on the figure 3.5.2.
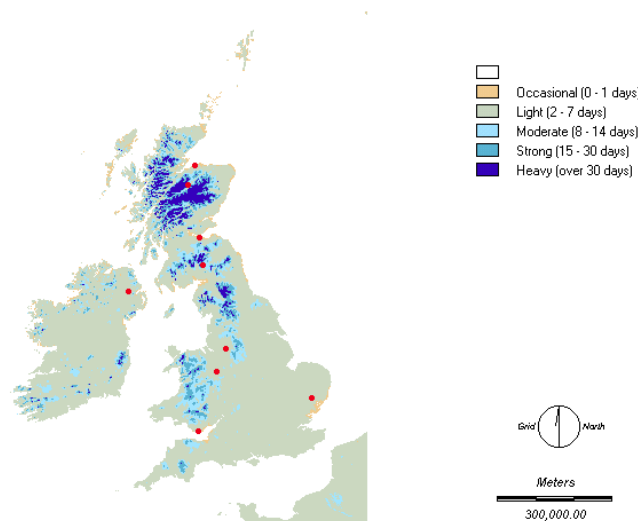

Figure 3.5.2 Annual number of in-cloud icing days in the UK and Ireland at ground level and the weather stations used in calculation. (Laakso T., Holttinen H. 2003)

Presented map was obtained by first examining the number of icing days at altitudes of 0m, 250m and 500m above sea level of nine weather stations. Further three altitude levels were interpolated to cover all area. Potential errors sources are local weather condition and low number of weather station. However L. Makkonen and K. Ahti as a result of Finland ice map investigation found that ice load change is not closely related to geographical location or elevation from the sea level, although local terrain has a major influence. (Makkonen L., Ahti K. 1995)

When comparing two presented maps different results can be seen. Possible causes can be local topography accounting, lower map scale. As can be seen presented map on figure 2.5.1 is not precise enough to make project special investment decision based on these results, it can be considered as indicative.

Most detailed icing maps are under development in those European countries, interested in cold climate regions sources utilization. However, ice detection is not included in the list of basic meteorological measurements. That is why such maps can be obtained by means of ice accretion models and necessary meteorological measurements, such as relative humidity, temperature and wind speed.

18

4. Ice accretion models

Icing in wind turbine blades is a great challenge to the successful wind energy implementation in cold climate regions. In order to prevent these consequences ice accretion should be predicted. COST Action 727 together with 13 European member states (Austria, Bulgaria, Czech Republic, Finland, Germany, Hungary, Iceland, Norway, Romania, Spain, Sweden, Switzerland, United Kingdom) and Japan currently targets at increasing the understanding and modeling of atmospheric icing structure. (Ronsten G., Dierer S. 2009)

As a result of weather conditions, height up to the earth level and temperature different kinds of ice can be accreted.

Currently several ice accretion codes exist in the international aircraft icing community such as LEWICE (U.S.A.), ONERA (France), DRA (UK), CANICE (Canada) and more recently CIRA (Italy) based on the physics of icing.

A numerical model of the amount and shape of ice accretion simulation has been under development in at the Technical Research Center of Finland (VTT) since 1991. (Makkonen L., Laakso T. 2001) The computers calculation capacity limits the progress of ice accretion modeling, it is too low to enable accurate weather predictions in a reasonable time together with the lack of accurate and full number of weather factors. Commercial programs and models for calculating ice induced loads are available. (Laakso T., Holttinen H. 2003) As long as new knowledge appears in the field of ice accretion structure and influences factors some development should be made with the programm. Wind turbine implementation experience shows that icing is also a problem even in climate with temperatures higher than in suggested as cold climate. Temperature near to 0 °C and freezing fallout result in the formation of glaze. Moreover unfrozen water, appeared after the heating, can run along the blade. In some cases it can be not a considerable problem, but the probability of this process should be taken into account.

4.1 TURBICE model

TURBICE simulates ice on a two-dimensional airfoil section in a potential flow field locating perpendicular to the airfoil axis. "Panel" method is used to obtain the numerical solution for the potential flow. Droplet trajectories are integrated from the steady-state equation of motion, using droplet drag coefficients of Langmuir and Blodgett (1946) and Beard and Pruppacher (1969). The integration begins ten chord lengths upstream of the airfoil section, and is carried out using a fifth-order Runge-Kutta scheme with an adaptive step-size control. The impact point is determined by linear interpolation between the 600 coordinate points, which define the airfoil section. The model simulates both rime and glaze icing. All angles of attack experienced by a wind turbine blade may also be calculated. The model can also simulate icing when the blade is heated. (Laakso T., Holttinen H. 2003)

In addition to the programm description simulation results comparison with the observation made during a field test at Pyhätunturi hill in northen Finland(67.01N, 27.13E, h=491m) is presented further. A case study was made on base of measurements on the 25th of April 2000. At the time icing situation were photographed. Obtained photos are compared to the simulated ice accretion for the same conditions. An example of the TURBICE input parameters are presented on the Table 4.1.1.
Presented meteorological data was obtained at the test site in co-operation with Finnish Meteorological Institute. Liquid water content LWC and median volume droplet MVD were obtained by using rotating multi-cylinder device(RMC) and Makkonen analysis method.

The ice accretion simulated using the input values in Table 4.1.1 is presented in Figure 4.1.1. The photo, made at the end of the simulated icing period is presented in Figure 4.1.1.
On the photo one part of the ice shape looks like "horns". However the horn shape structure is missing in Figure 4.1.1. There are several possible reasons for this difference explanation. First of all previous measurements at the site have revealed that the air can be significantly stratified at the top of the hill. It is then likely that the tip of the blade experiences variation in the air temperature. It is typical at the test site a

ground inversion appearance. The air temperature at the ground level deviates a few degrees from the temperature measured at height of the hub of a wind turbine.

Table 4.1.1 The TURBICE input parameters example. (Makkonen L., Laakso T. 2001)

TURBICE INPUT	
Meteorological wind speed	9,8 m/s
Air temperature	-3,5 °C
Rotating speed of wind turbine	42 rpm
Liquid water content of air (LWC)	0,14 g/m³
Median volume daimeter (MVD)	12,1 µm
Air pressure	96 kPa
Calculation time	30 min
Blade heating power	no
Chord	0,62 m
Profile coordinates (ABBOT)	0,62 m
Blade lift and drug coefficient	Naca63-213 files

Small fluctuations in the wind speed and wind direction all the time also appear. These factors are not taken into account in the TURBICE simulations.
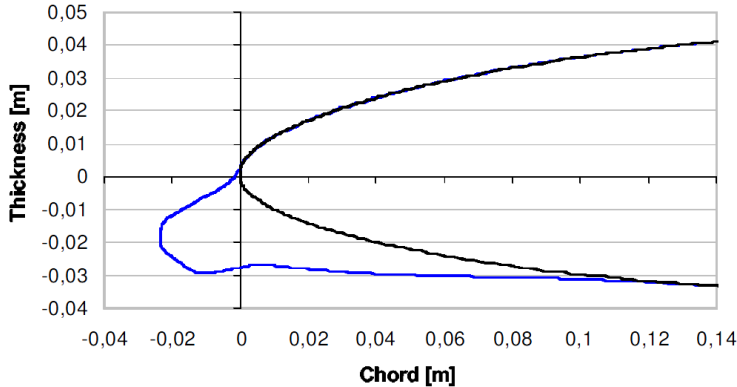

Figure 4.1.1 The simulated ice formation. Initial values according to Table 3.1.1(the case study) (Makkonen L., Laakso T. 2001)
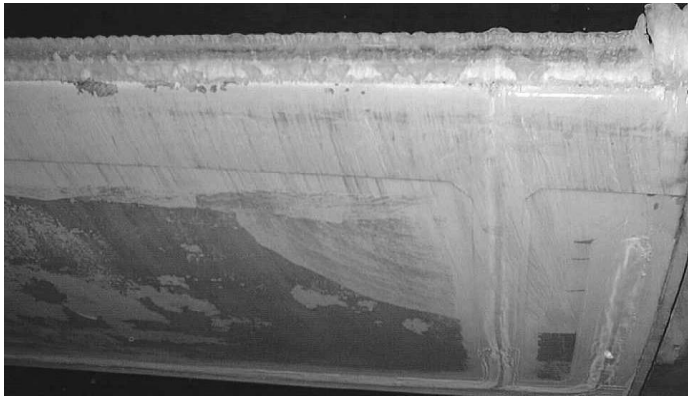

Figure 4.1.2 Photo of ice on a blade after the icing event in Table 3.1.1 (Makkonen L., Laakso T. 2001)

The effect of the air temperature on the ice shape is studied in the following, because there could be dependence between the air temperature and the difference in the shape of the simulated and photographed ice formation. Small temperature changes, which may take place during the RMC measurements, have a negligibly small effect on the measured values of LWC and MVD. Nevertheless, there are significant changes in the modeled ice shape because of the same small temperature variation, as shown in Figure 4.1.3. In Figure 4.1.3 the initial values, except the air temperature, are as in Table 4.1.1.
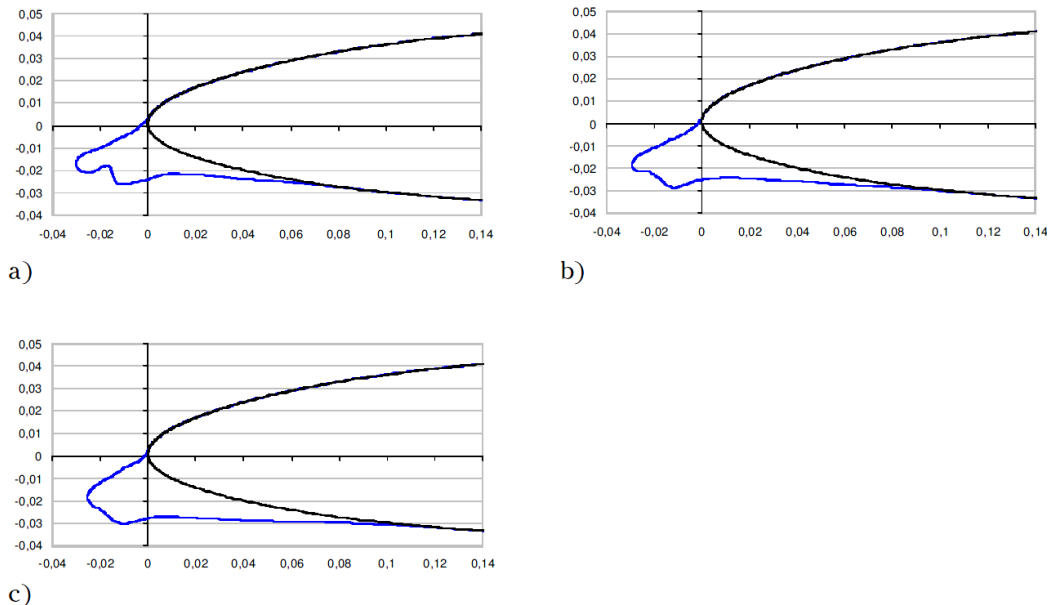

Figure 4.1.3 Effect of the surrounding air temperature a) T° = -2.4 C°, b) T° = -2.6 C° and c) T° = -2.8 C° on the shape of ice. Other model input as in Table 3.1.1 (Makkonen L., Laakso T. 2001)

TURBICE is able to calculate the heat balance of the heated wind blade. The TURBICE results were compared to those, obtained by using separate model. It uses cylinder and wedge analogies to determine the proper heating demand. (Makkonen L., Laakso T.2001) Comparison revealed some differences between simulated and calculated results. Heating systems and payback are considered further.

Comparisons with results of aircraft wing icing tests in a wind tunnel indicate that TURBICE simulations are realistic, except possibly at temperatures very close to 0 ℃. (Makkonen L., Laakso T. 2001)

4.2 LEWICE model

Another software, that can be useful for ice accretion and heating demand simulation, is Lewice 2.0. Lewice was developed by the icing branch at the NASA Glenn Research

Center in Cleveland, Ohio. The LEWICE base is an ice accretion prediction code that applies a time stepping procedure to calculate the shape of an ice accretion. (Wright W.B. 2002) The atmospheric parameters such as temperature, pressure, wind velocity, and the meteorological parameters such as liquid water content (LWC), droplet diameter, and relative humidity are specified as an input information and used to simulate the shape of the ice accretion. The software consists of four major modules:

1) flow field calculation,

2) particle trajectory and collision calculation,

3) thermodynamic and ice growth calculation,

4) modification of the current geometry by adding the ice growth to it.

LEWICE applies a time-stepping procedure to "build up" the ice accretion. The flow field and droplet collision characteristics are determined for the clean geometry. The particle trajectories and impingement points on the body are calculated from a potential flow solution that is produced by the Douglas Hess-Smith 2-D panel code included in LEWICE. Alternately and if specified the flow solution can be obtained from a grid generator and grid-based flow solver or read in as a solution file from this flow solver. The ice growth rate on each segment defining the surface is then determined by applying the thermodynamic model. When a time increment is specified, this growth rate can be interpreted as an ice thickness and the body coordinates are adjusted to account for the accreted ice. The ice growth rate on the surface body is calculated from the icing model that was first developed by Messinger. (Laakso T., Holttinen H. 2003) This procedure is repeated, beginning with the calculation of the flow field about the iced geometry, and continued until the desired icing time has been reached. (Wright W.B. 2002)

LEWICE can perform modeling of both dry and wet (glaze) ice growth. In addition to simulating the ice accretion, LEWICE incorporates a thermal anti-icing function. Calculation of the power density to prevent ice formation is performed by LEWICE. Two anti-icing modes are possible: running wet and evaporative.

It can generate not only anti-icing values, but also data about droplet trajectories, collection efficiencies, collision limits, energy and mass balances, ice accretion shape and thickness. Since potential flow cannot model stall or post-stall behavior, the

calculations are valid for unstalled rotor regions only. Ice accretion shapes for cylinders and several single-element and multi-element airfoils have been calculated using this software. The calculated results have been compared to experimental ice accretion shapes obtained both in flight and in the Icing Research Tunnel at NASA Glenn Research Center. The results of this comparison with the experimental database are presented further.

As an experimental data were taken the results of a wide variety of tests performed in the NASA Lewis Icing Research Tunnel (IRT) in recent years. Seven airfoils were selected for this comparison NACA0012, modified NACA23014, Large Transport Horizontal Stabilizer (LTHS), GLS305, modified NACA4415, NLF-0414, NACA0015. These airfoils and the accompanying ice shapes represent the complete set of publicly available data which has been generated in the IRT and digitized for single element airfoils.

The data is taken in the IRT by cutting out a small section of the ice growth and tracing the contour of the ice shape onto a cardboard template with a pencil. By means of a hand-held digitizer the pencil tracing is then transformed into digital coordinates. Some steps within this process which can potentially cause experimental error should be mentioned. Those which can be quantified by the current technique are the spanwise variability, the repeatability error, and errors involved in the tracing technique.

Available experimental data and LEWICE simulation results comparison shows that based on the overall assessment factor, the variation in the experimental data was 4.4% and the LEWICE predicted ice shape differs from the experimental average by 12.5%. (Wright W.B., Rutkowski A. 1999)
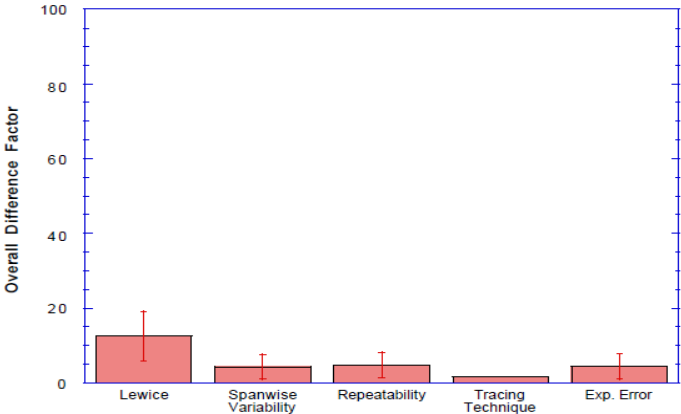

Figure 4.2.1 Overall ice shape variation compared to average experimental value. (Wright W. B., Rutkowski A. 1999)

5. Ice accretion effects

The problems because of the ice accretion are presented here.

5.1 Complete stop due to icing

In case of ice accretion on the turbine blade the machine should be stopped because of the human safety and equipment perfomance and lifelong. In some cases if the ice level is high blade can be even damaged under such load. As an example of wind turbine operation stop Äppelbo wind turbine in Sweden can be observed. (Homola M. C. 2005) 900 kW unit from NEG Micon is installed in this power plant, and it was stopped by icing for over 7 weeks in the winter of 2002-2003, as can be seen in Figure 5.1.1.
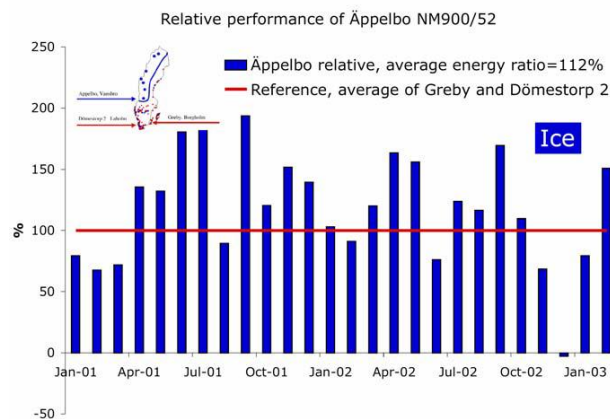

Figure 5.1.1   Relative performance of Äppelbo compared to two other wind turbines in southern Sweden, showing the result of complete stop due to icing in December 2002. (Homola M. C. 2005)

5.2 Aerodynamic parameters change

In order to be able to predict loads and energy losses for wind turbines operating under icing conditions it is necessary to qualitatively and quantitatively know the changes in the aerodynamic properties brought about by ice accretion on the blade's leading edges.

Because of the ice accretion on the turbine blade it's shape changes and therefore the aerodynamic characteristics changes, such as lift and drug coefficients and of course chord length. When growing ice accretion the drug coefficient is increasing and it leads to power coefficient change and therefore output power decrease.

During the European Wind Energy Conference in Ireland in 1997 were presented aerodynamics characteristics of turbine with different mass of ice accretion. Typical types of ice were removed from turbine blade and exact copies were made to add it further to blade in tunnel experiments. From these ice fragments two dimensional wind tunnel models were made. 300 kW turbine was investigated. NACA-4415 profile that represents the outer cross section of the rotor blade was manufactured with the original chord length.(Seifert H. 1997) Additional chord length can be up to 20% of the original chord length. In order to investigate the influence of the ice fragment shape and mass on the aerodynamic characteristics (lift, drug, moment coefficients) four different shapes were investigated.
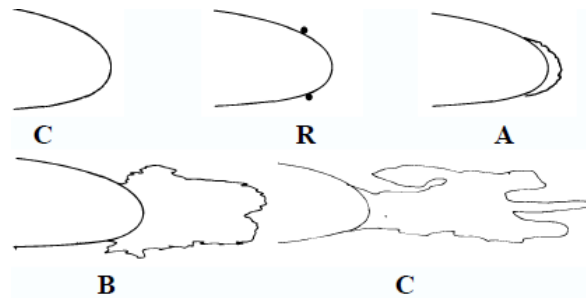

Figure 5.2.1 Typical catalogued leading edge ice cross sections. Clean Rough Type A Type B Type C (Seifert H. 1997)

The investigation was made based on the wind tunnel of the University of Braunschweig. Reynold's number was taken as 630 000. In the experiment under consideration the ice accretion investigated is similar to that collected from large turbines and the Reynolds number effect on the resulting coefficients is suggested negligible. Therefore the obtained results can be transferred to larger turbines. In the further chapters different turbine types and size ice accretion process is investigated. Angle of attack ranged from -10º to 30º. Figure 5.2.2 shows the wind tunnel view with the clean model.
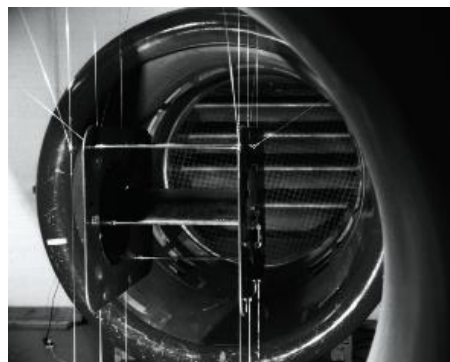

Figure 5.2.2 Open measurement cross section of the wind tunnel at University Braunschweig (Seifert H. 1997)

Stationary measurements reveal a remarkable difference between C type with 44% of ice and B type with 22% of ice.
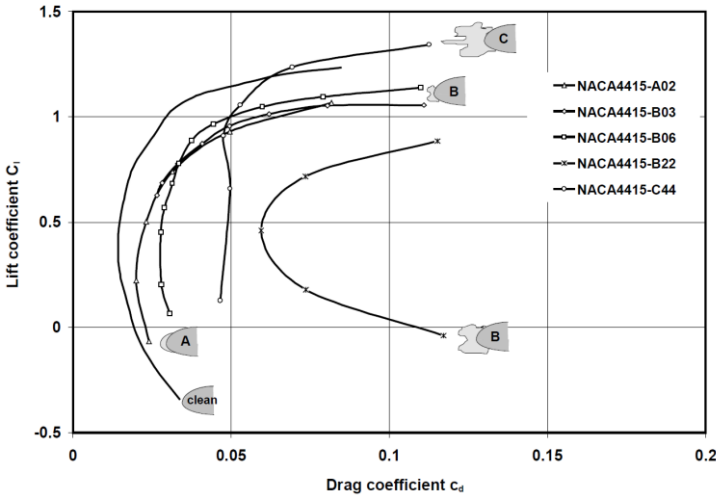

Figure 5.2.3 Lift coefficients versus drag coefficient for the various ice accretion models in the wind tunnel (Seifert H. 1997)

The explanation can be found in the ice shape analysis.

Lift coefficient versus angle of attack functions with different ice loads are presented on the Figure 5.2.4.

Instationary measurements were performed in order to investigate the stall region behavior in the icing condition. Although no significant changes were noted a shift of zero-lift angle of attack of the iced airfoil can be seen compared to the clean one as well as a lower amplitude of the maximum and minimum lift coefficient in the stall region for the iced section. The results are presented on the Figure 5.2.5.
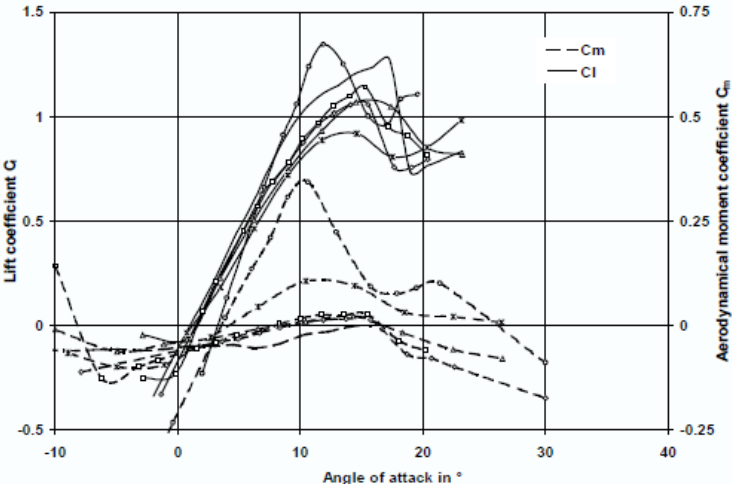

Figure 5.2.4 Lift coefficient versus angle of attack (Seifert H. 1997)

a) clean airfoil   b) airfoil with ice (22% type B leading edge ice)
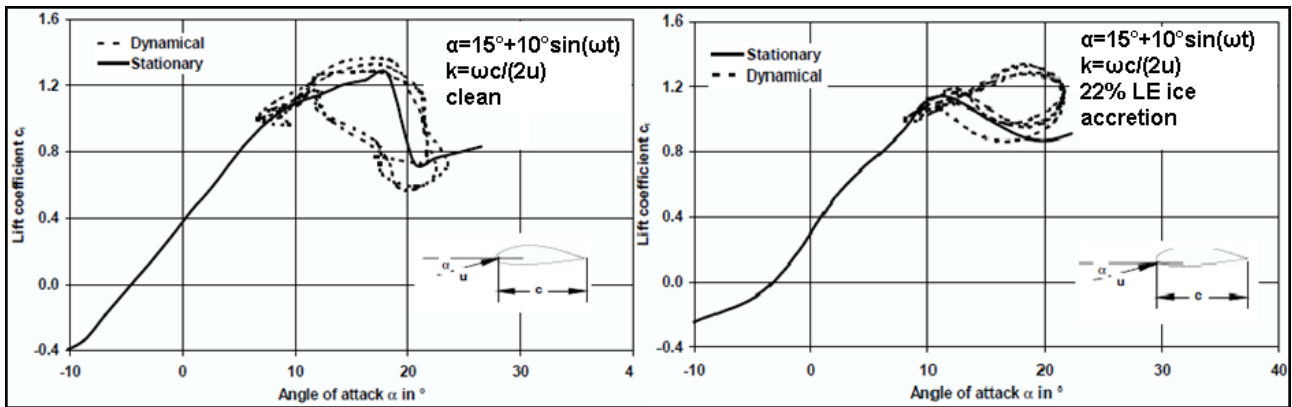
Figure 5.2.5 Stationary and instationary measurements with different ice load (Seifert H. 1997)

5.3 Energy losses due to ice

There are two methods of power losses estimation. First one is based on the power curve calculation with using of new iced blade experimentally obtained data. This method is observed further in presented work. The second one is based on the actual blade with ice and free of ice blade turbine power output records.

On a wind power plant in the town of Härnösand near to Stockholm, two HoloOptics Icing Rate Sensors was installed. The sensor without de-icing is indicating as more as 15 mm of ice is present on the probe. Härnösand sits on the Baltic Sea coast and during the winter it is often subject to icing due to southern winds with high humidity content. Among the measurements the wind speed and power outputs from the plant were measured. The wind speed and power output was sampled over ten minutes periods. The plant is a Vestas 600 kW installed 1997. (Westerlund R. 2011) The loss of power output is described as actual power output in relation to expected, nominal power output within the same conditions. If during the power plant operation the plant was stopped due to the lack of the wind these losses are not suggested as losses due to icing. Some errors can be brought by the wind estimation. In this case the wind speed was measured at a mast situated some 400 m from the wind power plant. The expected turbine power output is suggested dependent to the third power of the wind speed, although the real function is more complicated. Air turbulence can change with speed direction change. All these factors make contribution to the blurred relations on the curve. Figure 5.3.1 presents production losses due to ice accretion. The author by

adding diagonal P measured=P expected in order to achieve visual comparison of the obtained results. Original picture is available by (Westerlund R. 2011).
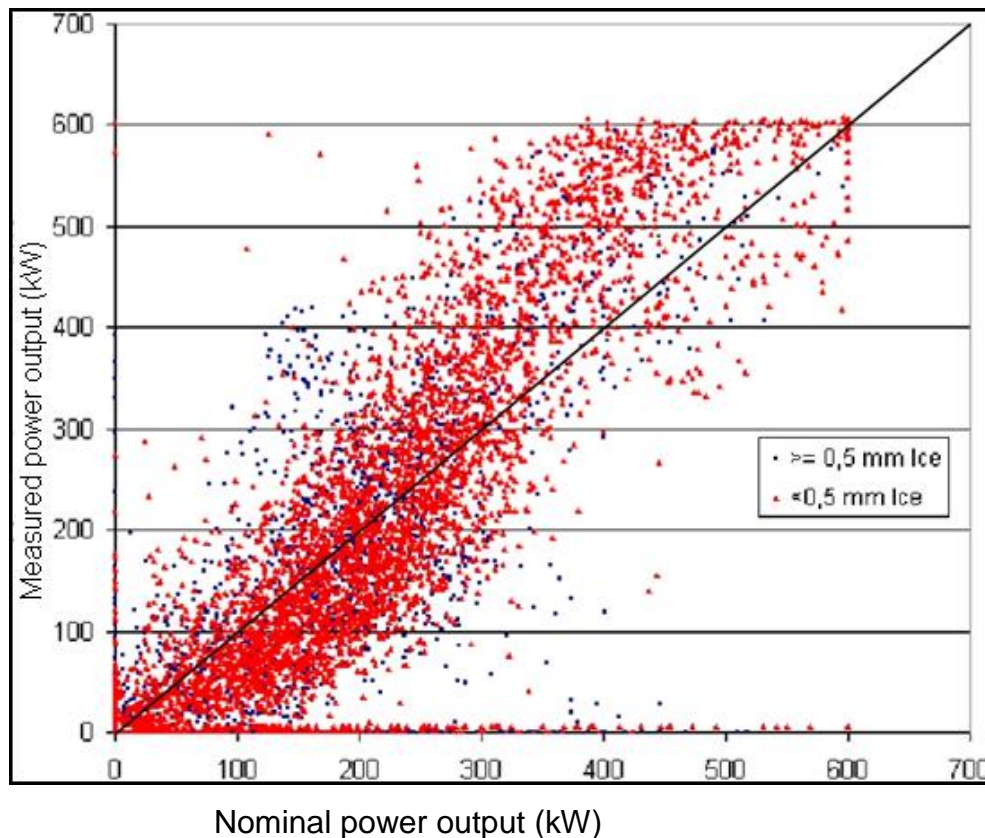

Figure 5.3.1 Measured and nominal power of the plant. (Westerlund R. 2011) Edition.

Moreover tests were made to investigate the influence of the quantity of accreted ice. There are results of the light and heavy ice influence. As it is shown on the figure 5.3.2 a) at the beginning of ice accretion there is even some excess of the expected power by obtained. As the ice gets thicker the losses become more notable. The closure of the plant at the end of the period on the figure 5.3.2 a) appeared due to the lack of the wind.

When ice thickness is more than 3-4 mm the plant was closed because the operation costs is higher than the value of produced energy. Nevertheless information obtained during plant operation under the heavy ice condition shows quite clear the losses level. During most of the time the reason for plant closure is the lack of the wind. In order to explain different level of losses in case of heavy and medium ice compare to light ice the quality of the ice should be mentioned. The blades were covered by rime ice during both periods shown in figure 5.3.2 a) and 5.3.2 b). Rime ice is more rugged than clear

ice. (Westerlund R. 2011) Rime ice will therefore cause more losses than clear ice at the same thickness.
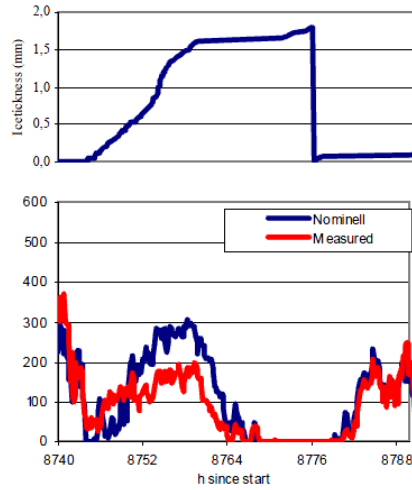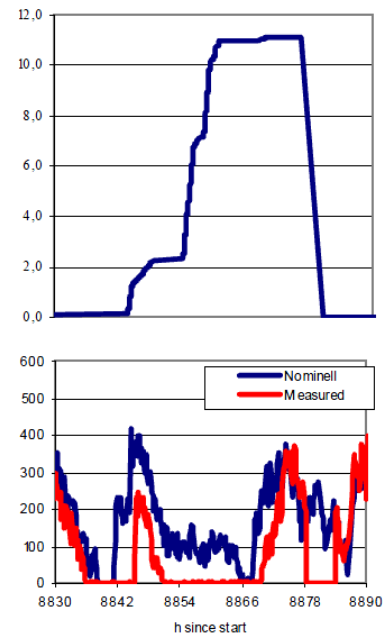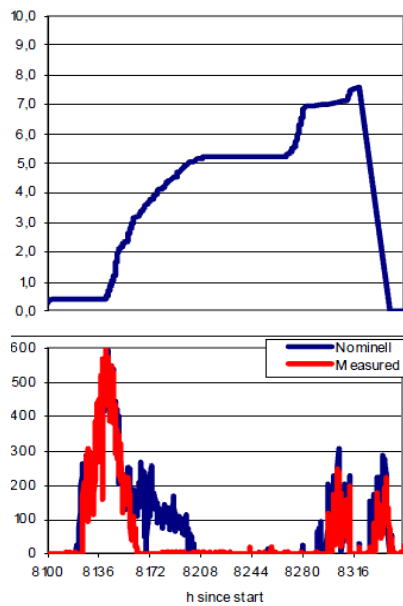

Figure 5.3.2 Power losses with light and heavy ice. (Westerlund R. 2011)

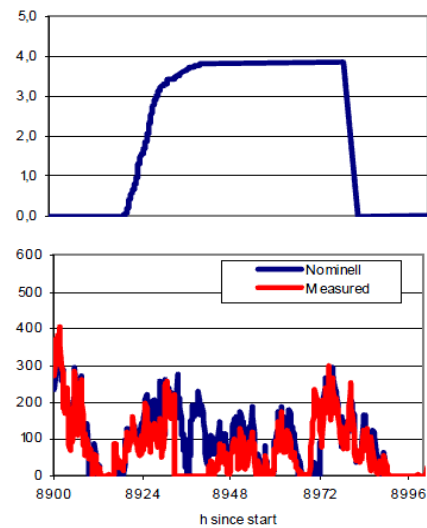In the figure 5.3.3 the blades were covered with clear ice.

Figure 5.3.3 Power losses with medium and heavy ice. (Westerlund R. 2011)

Moreover some results with economic point of view are presented. During January to March 2009 the plant in Härnösand had a loss of energy output of approximately 15 %

due to icing. Times when the plant was shut down due to risk for ice throw are included. More than 0,5 mm of ice was noted in approximately 505 hours out of a total of approximately 2 200 hours. During the rest of the year the icing accretion is very light and has no impact on the plant.

The loss of electric energy output over one year is estimated to approximately 5 %. The energy losses up to 35 % is due to the closing down of the plant due to the risk of ice throw. The electricity energy output is near to 1 200 MWh per year. Today its value is 45 000 € per year. The losses due to icing is 2 200 €. Over a 15 year period with 5 % interest that is 25 000 €. This is 3-5 % of the total installation cost. (Westerlund R. 2011)

5.4 Public safety

The ice fragments detached from the turbine blade can be quite large and should be taken into account.

Figure 5.4.1 Examples of ice fragments found near wind turbines, or taken from blades (Homola M. C. 2005)

Evidently that the risks of ice fragments throw and hit persons are greatest for service personnel who must approach the wind turbine, others can be at risk when the wind turbine is located near a road or recreation area.

In order to estimate the risk of a person being hit by a fragment of ice thrown from an operational wind blade one should consider the following influence factors:

  1) the probability that turbine blade will accrete ice,

  2) the probability that ice fragment will throw away from the blade surface, which depends on radial position on the blade and on blade azimuth. It may also depend on the rotation speed of the blades, as well as on blade pitch, blade profile and flexibility,

3) the place where the detached ice fragment lands, which is also the function of the radial position and azimuth at the time of becoming detached, and on the rotor speed and wind speed. The final speed of the fragment at the end of its trajectory is also of interest,

4) the probability that person will be in the risk area.

5.5 Ice throw distance

Although the lack of information and researches about the probability of ice fragments becoming detached from various parts of the blade, it is relatively easy to calculate the distance travelled and the fragment velocity in the end of the flight once it has become detached, assuming that it does not

break up in flight. There is quite rough method developed by Tammelin of the throw distance estimation, as described in equation 5.5.1.

$$d = (D + H) \cdot 1{,}5 \qquad (5.5.1)$$

d is the possible distance ice can be thrown,
D is the rotor diameter,
H is the height of the nacelle. (Homola M. C. 2005)

This equation can give just rough and first estimation of the probable distance with risk of ice fragments thrown.

Moreover there is more precise and complicated method, which has been developed as part of WECO and has been previously described by the authors in the (Morgan C., Bossanyi E. 1998) The model has been further developed and now includes the trajectory calculating in dependence of the following factors:

1) blade azimuth at the moment of the fragment releasing,

2) fragment radial location on the blade at the release moment

3) any radial sliping velocity developed by the fragment prior to release (the 'slingshot' effect)

4) turbine dimensions and rotor speed

5) fragment gravity force

6) fragment geometry and dimensions

7) aerodynamic drag force

8) aerodynamic lift force

9) mean downstream wind speed (Morgan C., Bossanyi E. 1998)

The released fragment will follow the whole range of trajectories depending in the mentioned factors. Monte-Carlo simulation generates the probability of each trajectories.

The acceptable level of risk should be determined. This is subject to case specific factors such as ease of access, nevertheless a suitable level may be $10^{-6} \frac{strikes}{\text{year·m2}}$ which is the typical probability of lightning strike in the UK. (Morgan C., Bossanyi E. 1998)

According to the Austrian experience when driving 10.000 km on a highway one obtain the risk for event of death of 10^{-4} for a single person, while the probability of death when working in the office is 10^{-5}. (Krenn A. 2011b)

In order to avoid mentioned risk the following actions can be done. Warning signs for ice throw danger indicating have to be placed on each entrance point to the wind farm area with a minimum distance of 250 m to the turbines. One single wind turbine has to be equipped with an ice detector for automatic stop of all turbines in case of risk of icing occurring. Wind turbine operation when there is ice accretion on blade is not allowed – turbines have to be stopped automatically. Automatic Re-start of the turbines during danger of icing is not allowed. Manual Re-start of wind turbines after automatic stop due to icing is only allowed under on-site attendance of operational staff. (Krenn A. 2011a) Evidently presented information corresponds to the local place and local case, but the scope of the risk can be observed.

5.5 Maintenance management

Maintenance management problems can be divided on blade and tower dynamics investigation.

5.6.1 Blade dynamics

Additional ice masses accretion on the blades can lead to blades damage and overload. In order to escape it blades equipped with the heating systems (ice

preventing systems are considered in the further chapters) or turbine has to be stopped.
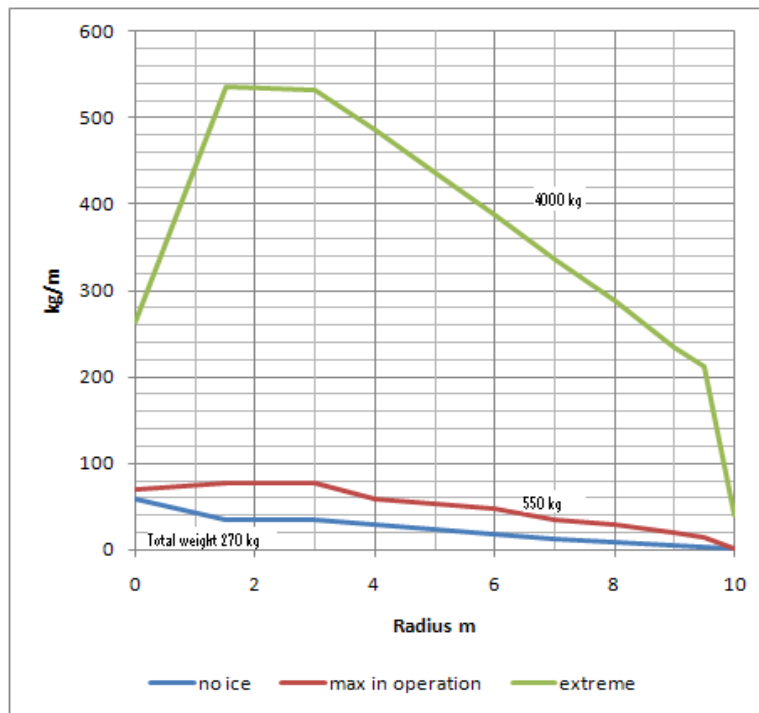

Figure 5.6.1.1 The mass of a typical rotorblade with the additional ice mass. (Böhmeke G. 1992)

V. Carlsson in (Böhmeke G. 1992) supposes that long lasting turbine operation under ice condition decreases the level of this problem. Moreover activated by severe blade vibration switch protects turbine.

5.6.2 Increased fatigue caused by imbalance

Ice accretion is not symmetrical with turbine blades, every blade has different ice load. It leads to imbalance and increase in the loads imposed on every components of the turbine. Fatigue load causes a shortening of the lifetime for all components.

6. Ice detection

Ice detection is a critical measurements wind turbine operation in cold climate. The main purposes of the various types of available ice detectors are to indicate or measure the assumed ice accretion. The time of ice accretion is necessary to know in order to calculate heating energy and therefore due to ice losses. An ice detector is recommended according to the site measurements. Although in present time there is

no verified and fully reliable ice detectors equipment in the near time ice detection technology is expected to be improved due to increased wind energy business development.

6.1 Ice detection methods

According to climates conditions and ice detectors purpose various ice detecting methods are suitable. Icing can be detected either directly or indirectly. Ice accretion cause some property change, it is detected in the direct method. Mass, reflective properties, electrical or thermal conductivity, dielectric coefficient and inductance change are to be observed in the direct methods. The indirect methods are based upon detecting the weather conditions that lead to icing. Humidity and temperature are among them. Also detecting the effects of icing can be made by a reduction in power production estimation. The next methods step is icing occurring location determination by means of a model, either empirical or deterministic. The methods available for detection of ice are listed further. The sensor types listed here are described according to the measurement principle, though the sensor types have many references associated with them. (Homola M. C., Nicklasson P. J. 2006)

1) Direct detection: damping of ultrasonic waves in a wire, damping of ultrasonic waves on the wing surface, inductance change, impedance change, capacitance change, temperature rise with heat, temperature curves when heat is applied to small areas, resonant frequency of a probe — magnetostriction, resonant frequency of a probe — piezoelectric, microwave waveguide, reflected light from inside, fiber optic cable with special clad, flexible diaphragm, mechanical resistance to piezoelectric expansion, piezoelectric pressure sensor to detect ice and turbulence, reflection of polarized infrared light, infrared spectroscopy, ice blocking an exit hole is detected, reflective light sensor, stereo imaging from web cameras, ultrasound system from inside the blade, surface impedance and temperature, ice collecting cylinder, surface acoustic wave sensor.

2) Indirect detection: dew point and temperature, actual power output vs. predicted from wind speed, anemometers with and without heating, frequency of generated noise, change in blade resonant frequency.(Homola M. C., Nicklasson P.J. 2006)

German company Infralytic developed new type of ice detector, based on the light emitting diodes (LEDs), fibre optics, and light refraction on the wind turbines' blade surface. Detector is able to distinguish between glaze, rime ice, dirt.

In the Japanese Kanagawa Institute of Technology new detection method successful experiments were made. Ice accretion was detected be means of reflection and absorption of infrared light on the model surface. (Ronsten G. 2008)

6.2 Ice detection sensors

Sensors for measuring wind speed (anemometer) and wind direction (wind vane) are the very important components in wind energy technology. Ultrasonic instruments provide information about wind speed and direction, while cup anemometers utilization demands additional equipment such as vane anemometers for wind direction detection. Heated anemometers can be used, but under sever ambient conditions they can fail. Pair of heated and unheated anemometers is also used. The ice detection parameter is each anemometer output information deviation under icing conditions. Since both anemometers output data is the same under normal condition. When using nacelle anemometer obtained wind data in combination with ambient temperature and analysis of wind turbine performance are considered. Actual turbine power deviation from expected is the ice accretion parameter.

6.3 Ice detectors requirements

The best place to locate ice detectors is on the blade itself and close to the blade tip. The rate of ice accretion depends on the relative velocity of the supercooled particles, the highest velocity occurs exactly on the blade tip. The outer ends of the blades sweep a larger volume and collect water or ice from the entire volume. Measurements made in Pori (Finland) shows that the number of in-cloud icing periods on the 84 m altitude is 6 times the number on the 62 m altitude. (Homola M. C., Nicklasson P.J. 2006)

During the winterwind conference in Sweden some results were presented of the experiments with stationary ice sensors and moving turbine blade under the ice conditions. (Carlsson V. 2011)

One of the study aims is to find a correlation between the stationary sensors data and ice accreted on the rotor blade. Ice appearance on the blade was detected by the deviation in the power curve. If the ratio between real and expected power is less than 0,85 the ice assumed to be accreted. Two sites were investigated. Stationary ice sensor was installed at site A and two different type sensors were installed at one of the nacelles. Several multi megawatt turbines were investigated. There are no anti-icing and de-icing systems.

Some interesting results were obtained by comparison of modeled ice accretion and data obtained by the stationary sensor (site A) and blade installed sensors (site B). Simple model of ice accretion prediction is used, according to the humidity and wind speed the ice accretion is assumed, the amount of ice is calculated either with 5.3.1 (temperature below freezing) or 5.3.2 (temperature above freezing) equation according to ISO-standart. (Carlsson V. 2011)

$$\frac{dM}{dt} = 0,11 \cdot A \qquad\qquad (6.3.1)$$

$$\frac{dM}{dt} = 0,04 \cdot A \qquad\qquad (6.3.2)$$

Table 6.3.1 Icing condition estimated. (Carlsson V. 2011)

Parameter	Site A		Site B	
	Measured	Model	Measured	Model
Active icing time, %	15,8	28,5	23,2	27,8
Maximum ice load [kg/m]	3,05	5,53	11,4	16,8

Model overestimated load and ice time can be clearly seen from table 6.3.1. Nevertheless icing time start can be predicted quite precise.

When comparing results with those detected from the power output decreasing the lack of information should be mentioned. Often turbine was stopped because of the heavy ice accretion. Figure 6.3.1 shows the correlation obtained. In most cases icing events were caught by sensors, but still with less than 100% precise. Red rounded area on the Figure 6.3.1 illustrates this event. Green line shows that turbine production power corresponds to the ice-free condition. However sensors show icing accretion.
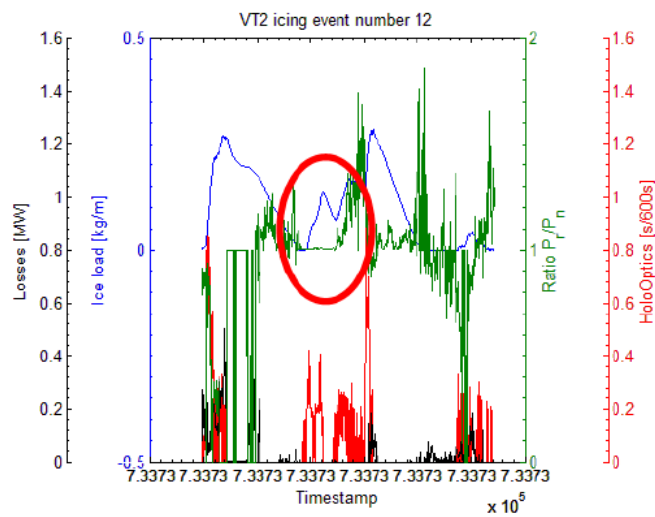
Figure 6.3.1 Sensors data and production losses correlation. (Carlsson V. 2011)

Among the requirements ice detectors ability to detect ice over a large area of the turbine blade should be mentioned. Ice does not occur at the same location in the blade. Glaze icing could be accreted over large areas of the blade, with water running back and freezing away from the leading edge. Generally rime icing occurs on the leading edge, around the stagnation point, but depending in the angle of attack the exact location can vary. Also ice fragments can be detached from the blade. It can result in some area of the blade clean and some iced. Ice detection sensors have to detect ice at more than one or two points.

6.4 Ice detection problems and challenges

Among the ice detection problems detectors response time has to be mentioned. Ice accretion on the wind blade should be detected as soon as possible because of the increased heat transfer as a consequence of turbulent airflow over a rough iced blade surface. Therefore the heat demanded for ice melting become higher. Also important question is the melting cycle, the heating power can be insufficient to remove all the accreted ice or the already melted ice freezes again after heating period. (Laakso T., Holttinen H. 2003) Because of the listed problems combining an ice detector and a humidity and temperature sensors have been investigated. When the temperature is below zero and relative humidity is over than decided limit (90% for example) it is assumed that ice occurs. Ice accretion is complicated process and there are many influence factors. According to meteorological data and experiments ice occurs sometime with the conditions unexpectedly. In some cases ice should appear with the

probability of 100% under the observed conditions but it does not appear. Ice detection reliability and precise are still question under consideration.

7. Anti-icing and de-icing systems

There are two main icing mitigation strategies: anti-icing and de-icing systems (ADIS). Anti-icing system prevent icing accretion on the blade, while de-icing system removes accreted ice. Both strategies can be divided into two main methods: passive and active. Passive methods utilize the advantages of the blade surfaces in order to eliminate ice accretion. Active methods use an external system and require external heat or energy supply.

Blade heating system can be profitable if there is frequent icing or high safety requirements. In order to estimate the heating system profitability one should know wind sources, energy demand (wind turbine operation time), icing frequency and load, icing time and heating system energy consumption, electricity cost. Also as it was investigated in most cases ice accrete on the blade leading edge, so it is necessary to heat not the whole blade inside, but just part.

7.1 Active ADIS methods

The relative cost of ADIS is highly dependent of the location, ice and weather characteristics, wind sources and utilization. The average energy consumption can be suggested as 6 to 12% for electrical anti-icing, of 100–220 kW turbines, and 10 to 15% for warm air ADIS. Some studies estimate power consumption up to 2% of nominal power output. In global values, the ADIS consumption is assumed to be in a range from 1% to 4% loss of annual energy production, depending on icing severity. ADIS installation cost is estimated to be up to 5% of the 600 kW turbine, the large is turbine capacity the less became this percentage, evidently. De-icing system energy demand is large because detaching already exist huge amount of ice is more power-consuming.

Electro thermal heaters

Electro thermal is the most popular among active de-icing methods. Kelly aerospace, EcoTemp, VTT developed electro thermal de-icing systems based on the electricity conversion to heat and special heat-conducting surfaces. The base idea is to create the water layer between the ice and the surface. In order to control the operation of the heating system ice detector and blade surface temperature are used. Moreover additional temperature sensors are installed to protect the blade from damaging because of overheating. Finnish JESystem recent results estimate energy consumption up to 0.5 kW/m, which is approximately 5% of the power output. (Parent O., Ilinca A. 2011) Usually it is necessary to keep heating after the icing event during 15-30 minutes.

Advantages of the method:
1. Comparatively simple and widely spread.
2. If considering the profitability of wind energy production the needed energy is small.
3. Thermal efficiency is close to 100% due to direct heating.
4. Energy demand does not increase with the turbine capacity increase.
5. Comparatively low energy consumption.

Disadvantages of the method:
1. Despite of the product availability there is no mass production.
2. The technology prototype level because of the limited market.
3. Even one heating element failure leads to the whole system imbalance.
4. Run-back water should be managed. If not it can reach blade cold area and re-freeze. Further it can lead to the «horn» appearance on the blade.

Warm air and radiators

The method main idea is still to create water film between ice and surface, but now by means of blowing warm air inside the blade. Blowers locate in the blade root. Internal blade volume is divided into two sections so the circuit for air is created. Hot air is going throw one section, cold air is sent to the heating system to another blade section. This closed circuit reduces the needed energy, since the initial air temperature is higher than outside one. The process efficiency can be improved if using hot waste air from machinery.
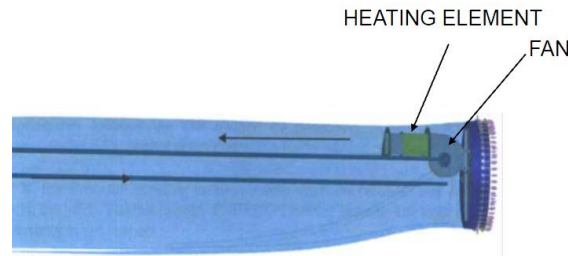
Enercon

Figure 7.1.1 Enercon ADIS(Gedda H. 2011)

Advantages of the method:

1. Comparatively low energy consumption can be achieved.
2. There is no effect on the leading edge surface and the blade's aerodynamics.
3. The system has not any effects on the lightning protection system.

Disadvantages of the method:

1. High power consuming when high speed velocity and low temperatures.
2. Hot air demand increase with the turbine capacity increasing.
3. Thermoset composites maximum operating temperature should be controlled.
4. Thermo efficiency is low because of the large amount of air should be heated before desired temperature is achieved. Blower usually is located near to the blade root while the highest heat fluxes are needed at the tip of the blade.
5. Such system works when ice already accretes on the blade surface, so the hazard of falling ice fragments should be taken into account.

As it was mentioned the heating system application profitability depends on many local factors. As an example Swiss experience can be mentioned. Additional energy obtained due to heating system installed is investigated. The whole icing period can be divided into two: meteorological ice and instrumental ice period. The optimal time for heating system to start is exactly meteorological ice time. Ice melting during the instrumental ice time demands more energy.
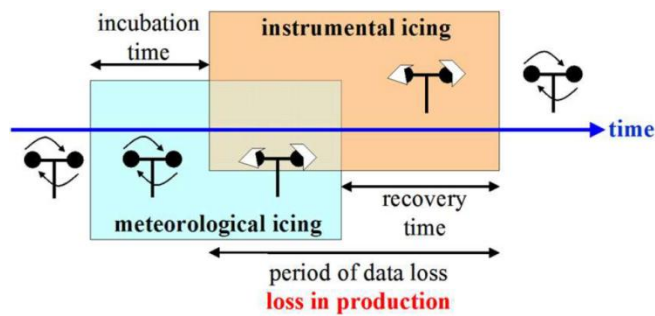
Figure 7.1.2 Analysis of meteorological and instrumental icing period. (Cattin R. 2011)

Turbine stops when ice is detected and is heated during 3 hours, after that automatically restarted. It was assumed that without heating system turbine should be stopped when ice is detected and automatically restarted when the average temperature is above 2°C during 6 hours. Without heating system losses are up to 10%, blade heating energy losses is approximately 0.4%, energy losses because of turbine stop during heating is up to 3%. Blade heating system gives up to 7% energy saved. In this particular case heating system application appeared to be profitable. (Cattin R. 2011)

Both systems operation time should be controlled to avoid blade overheating, high energy consumption. The simplest option, if ice events are rare, is to stop the turbine operation or continue to operate. The second option is to restart turbine automatically or after visual observation. Unusual strategy is to keep heating system working all the time, but it increases energy consumption. Heating control system can react on the blade surface temperature, it also helps to avoid blade overheating.

Flexible pneumatic boots

Flexible pneumatic boots remove ice from blade surface by breaking after surface inflation. In the normal mood tubes comply the blade surface. Generally 6 to 13 mm of ice accreted give start to de-icer to inflate with the compressed air. After few seconds ice detaching is achieved and further accretion prevented, and the ice fragments are removed from the blade surface be centrifugal and aerodynamic forces. De-icer is than deflated.

Advantages of the method:

1. Low energy consumption.
2. During laboratory tests good results were achieved.

Disadvantages of the method:

1. Field-landed tests have to be made.
2. Aerodynamic characteristics can be disturbed because of the drag coefficient increasing.
3. Maintenance requirements during lifelong period can be expensive.
4. High centrifugal loads at the outer radius of the pneumatic system will inflate itself or has to be divided in short sections.
5. Detached ice fragments hazard should be taken into account.

The same idea is used in electro impulsive method. Magnetic field is created between spiral coil and the thickness of the profile, further the vibration of the surface breaks the ice. It is new technology, which has not been tested yet on wind turbines. The potential problem is still ice fragment throw.

7.2 Passive anti-icing methods

In case of slight ice accreted and rare ice events it is feasible to use passive anti-icing systems.

Special coatings

Ice-phobic coatings prevent ice from adhesion to the surface due to their anti-adhesing properties. Super-hydrophobic coatings prevent water from remaining on the surface due to their repulsive properties. Among such materials epoxy or polyester matrix composites reinforced with glass or/and carbon fibre can be mentioned. Moreover polyester and glass remain more often used due to low price. Nano-composite coatings are now of big interest. They create high contact angle between blade surface and water. Blade surface can be covered with a chemical liquid, which make surface hydro-phobic. Such method demand special applications and a lot of maintenance. It is pollutant and the surface should be recovered with the liquid quite often.

Advantages of the method:

1. Low cost.
2. There is necessity in special lightning protection.
3. The whole blade surface protection.
4. If coating is used with the active anti-icing system it reduces energy consumption.

Disadvantages of the method:

1.   Ice throws away and it is still problem.

2.   After a short period of time coating becomes porous and should be changed. (Parent O., Ilinca A. 2011)

According to the list of lab and field-tested experiments coating alone does not prevent ice accretion. (Parent O., Ilinca A. 2011) New coating experiments were made based on the Fraunhofer IFAM Institute. Optimal balance of hydrophobicity, roughness and available bonding types at the surface were achieved with Fluor- and silicone- modified coatings. (Sell S. 2011) Although, no field-tested experiment were made yet.

Parameter	Unmodified top coat	Passive anti-ice coating
Water contact angle [°]	82	124
Roughness Ra [μm]	0.17 (±0.01)	0.64 (±0.07)
Pictures of the ice rain test		
Description of result	Ice formation after rain at -5°C	• Reduced ice formation due to improved water run-off • Ice adhesion reduced
Limitation	Rime ice accretion is not reduced	

Figure 7.2.1 Investigations of the influence of key parameters on the icing behavior of surfaces. (Sell S. 2011)

Black paint

Black color characteristics heats the cover more than white one, so the blade surface are warm and ice accretion is prevented.
Advantages of the method:

1.   Described method can be useful in areas where ice is slight, infrequent, winter solar intensity is high at low altitudes and the icing period is followed by the temperatures above 0°C. In Canada and Finland this method application shows notable good results. (Parent O., Ilinca A. 2011) (Böhmeke G. 1992)

Disadvantages of the method:

1.   Blade surface overheating during the summer if such appears.

8. Mathematical description of the design methods

Technical methodology of aerodynamic, economy parameters calculations are presented in this chapter.

8.1 Model of aerodynamic parameters calculation

The theory of moments applied to the blade elements (BEMT) is considered as classical for the power factor and other blade characteristics calculation. The method base are momentum balance on a rotating annular stream tube passing through a turbine and examination of the forces generated by the airfoil lift and drug coefficient at various section along the blade. Thus a series of equation can be obtained. They can be solved iteratively.

BEMT detailed explanation can be found in (Ingram G. 2005) and (Manwell J.F., McGowan J.G et al. 2009).

8.2 Description of the initial data

Sets of initial data should be obtained in order to calculate blade characteristics. Three-blade horizontal wind turbine is considered in this research, however the number of blade can vary. The blade length is divided into N sections. Chord length *c*, rotation angle *γ*, blade profile in the cross section are specified. According to the RISØ test turbine data (Schepers J.G., Brand A.J. 2002) these blade characteristics were taken as working for the search.
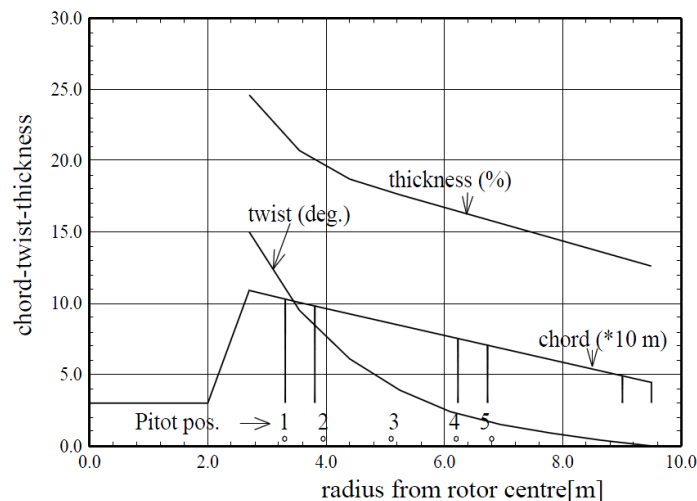

Figure 8.2.1 RISØ, The planform data for the test blade. (Schepers J.G., Brand A.J. 2002)

Based on figure 7.2.1 data $c(r)$, $\gamma(r)$ functionss were obtained.

The profile section is NACA 4415. This profile selection is explained by the profile obtained characteristics when the blade is with ice accreted.

8.3 Calculation of the induction factors and the relative angle of attack

There are list of BEMT assumptions:

1.   There is no aerodynamic connection between the elements of the blade. In other words, each element or section of the blade can be examined separately.
2.   The forces acting on the elements of the blade are determined only by lift and drag coefficients.
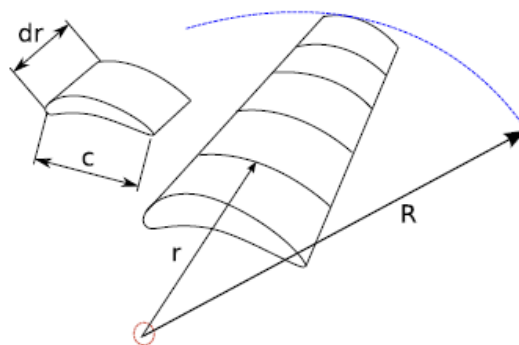

Figure 8.3.1 The blade element model. (Ingram G. 2005)

Each blade element experiences a slightly different flow as it has own rotation speed ($\Omega \cdot r$), chord length (c), twist angle (γ). After each element characteristic calculation the overall performance can be determined by numerical integration along the blade.
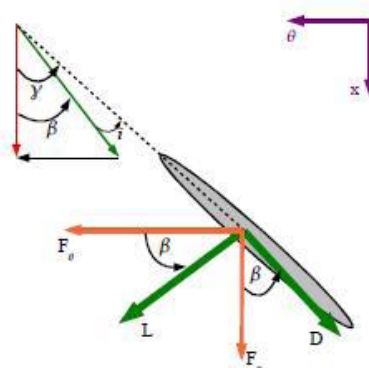

Figure 8.3.2 Blade section flow angles and forces. (Ingram G. 2005)

Tip loss correction factor should be taken into account, because originally BEMT does not consider the influence of vortices shed from the blade tips into the wake on the induced velocity field.

The following two basic equations were used in order to calculate blade characteristics:

$$\frac{a}{1-a} = \frac{\sigma[C_L sin\beta + C_D cos\beta]}{4Q cos^2\beta} \qquad (8.3.1)$$

$$\frac{a'}{1-a} = \frac{\sigma[C_L sin\beta - C_D cos\beta]}{4Q\lambda_r cos^2\beta} \qquad (8.3.2)$$

a −axial induction factor,
a' −angular (tangential) induction factor,
$\sigma = \frac{Bc}{2\pi r}$ − local solidity, where B − number of blades,
c −blade chord,
r − radial direction, distance from the blade root to the blade element under consideration;
β −relative angle of attack,
λ_r −local tip speed ratio,
$Q = Q_1 \cdot Q_2$ −resulted losses, $\qquad (8.3.4)$
Q_1 −tip loss correction factor, it can be calculated by using equation:

$$Q_1 = \frac{2}{\pi} cos^{-1}\left[\left\{exp - \left(\frac{B\left[1-\frac{r}{R}\right]}{2(r/R)cos\beta}\right)\right\}\right] \qquad (8.3.5)$$

When determing the blade radius dividing on the sections it is important to suggest the last section less than the actual blade radius. As can be seen from 8.3.5 equation if $r = R$ then $Q_1 = 0$ and 8.3.1 equation become equal to infinity. In order to escape such problem the author suggests the last blade point $r = 9,4$ when the total blade radius is 9,5m.

Q_2 −hub losses:

$$Q_2 = \frac{2}{\pi} \cdot cos^{-1}e^{\left[-\left[\frac{Br\left(\frac{1-R_{hub}}{r}\right)}{2R_{hub}cos\beta}\right]\right]} \qquad (8.3.6)$$

R_{hub} −hub radius,
C_L, C_D − the lift and drug coefficients respectively, they are the main experimental parameters of the blade profile.
These coefficients vary depending on flow velocity, in other words, on Reynolds number and angle of attack i. Those coefficients characterize blade profile.

Presented research considers characteristics, shown on figure 8.3.3. They were obtained by means of tunnel experiments. Blade section without ice and with different

levels of ice was investigated. On the Figures 8.3.3 and 8.3.4 only characteristics under investigation are shown.
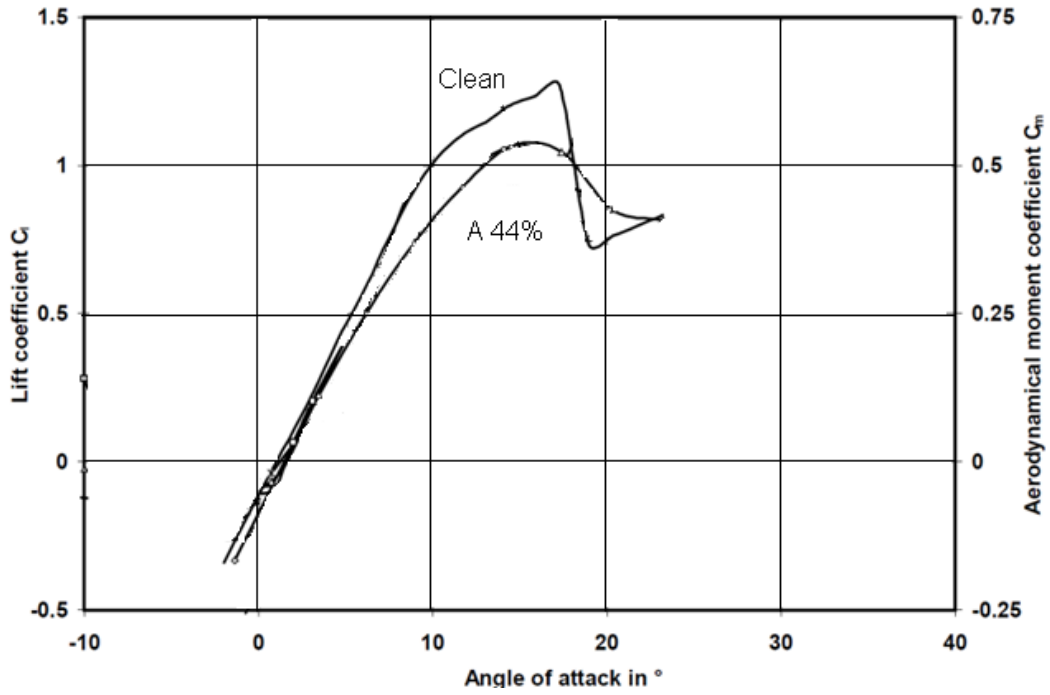

Figure 8.3.3 Lift coefficient versus angle of attack. (Seifert H. 1997). Edition.
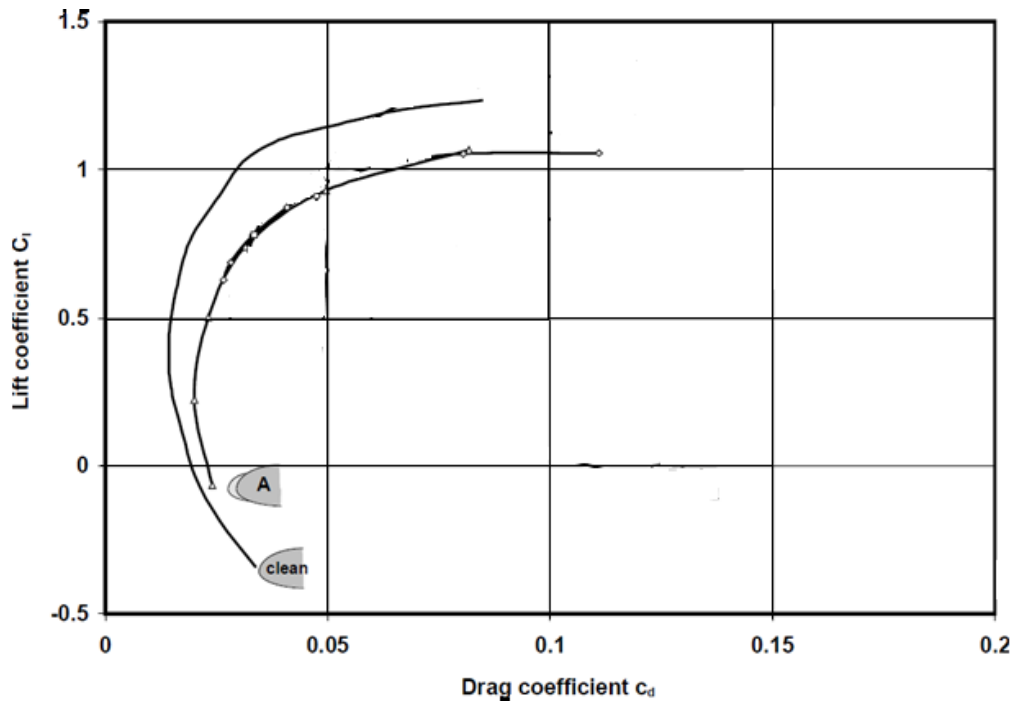

Figure 8.3.4 Lift coefficients versus drag coefficient for the various ice accretion models in the wind tunnel. (Seifert H. 1997). Edition.

Section where lift coefficient is almost a linear function of angle of attack is called workspace. The drug coefficient assumes minimal values in this area. When angle of

attack reaches certain value further angle of attack increasing leads to the lift coefficient decreasing and drug coefficient increasing. In order to avoid operation in this area blade twist control system can be applied.

Moreover, when the induction factor is greater than 0,4 the basic BEMT becomes invalid. This occurs when turbine operates with high tip speed ratio. More flow entrains from outside the wake, the flow behind rotor slow down, while the thrust on the rotor disk continue to increase. In order to compensate this effect a corrections to the rotor thrust coefficient should be calculated. (Moriarty P. J., Hansen A. C. 2005)

$$C_T = \frac{8}{9} + \left(4Q - \frac{40}{9}\right)a + \left(\frac{50}{9} - 4Q\right)a^2 \tag{8.3.7}$$

New equation for induction factor is the next (Moriarty P. J., Hansen A. C. 2005):

$$a = \frac{18Q - 20 - 3\sqrt{C_T(50 - 36Q) + 12Q(3Q - 4)}}{36Q - 50} \tag{8.3.8}$$

Basically calculations start with the choosing of wind wheel diameter according to the wind conditions and the output energy requirements. Assuming power factor for modern three-blade wind turbine approximately equal to 0,4 and the total electrical and mechanical efficiency equal to 0,9 the radius of the blade can be calculated by using the next equation:

$$R = \sqrt{\frac{2P}{C_p \eta \rho \pi V^3}} \tag{8.3.9}$$

P −output electric power of wind turbine,

ρ −air density, assuming under normal conditions equal to 1,225 $\frac{kg}{m^3}$

V −wind speed on the tower height.

Presented article considers blade with 9,5 m radius, according to RISØ data.

Then tip speed ratio λ should be chosen. For three-blade wind turbine it is assumed equal to 4-6. (Ingram G. 2005) Blade should be divided into 10-20 sections, the calculations accuracy depends on this number of sections. Presented article considers 14 sections.

At the very beginning of the calculations the relative angle of attack, induction factors are determined by the equation:

$$\beta = 90° - \frac{2}{3} arctan\left(\frac{1}{\lambda_r}\right) \tag{8.3.10}$$

$$a = \frac{\sigma'(C_L sin\beta + C_D cos\beta)}{\sigma'(C_L sin\beta + C_D cos\beta) + 4Q cos^2\beta} \tag{8.3.11}$$

Equation 8.3.11 is going from 7.3.1. (Moriarty, P. J., Hansen, A. C. 2005) suggests the next equation for angular induction factor calculation:

$$a' = \left[-1 + \frac{4Q sin\beta cos\beta}{\sigma'(C_L cos\beta - C_D sin\beta)}\right]^{-1} \tag{8.3.12}$$

Lift and drug coefficients are determined from the chosen profile experimental data, the resulting angle of attack $= \beta - \gamma$, where γ −the given twist angle of the blade section under examination. Thus the first data is obtained and the iterative process begins. The relative angle of attack further is determined as follow:

$$\beta = arctan\left(\frac{\lambda_r(1+a')}{1-a}\right) \tag{8.3.13}$$

New angle of attack, induction factors values are calculated as previous ones. They should be compared with those obtained in previous step:

$$\varepsilon_a = 1 - \frac{a_n}{a_{n+1}} \tag{8.3.14}$$

$$\varepsilon_{a'} = 1 - \frac{a'_n}{a'_{n+1}} \tag{8.3.15}$$

The iterative process is going on while the calculation accuracy for both parameters is equal to 5%. This calculation process should be carried out for all sections along the blade. As a result the induction factors $a = a(r), a' = a'(r)$ and the relative angle of attack $\beta = \beta(r)$ are obtained.

8.4 Calculation of the power coefficient

Power coefficient is the ratio of produced aerodynamic wind power to the input power of wind flow. The power coefficient can be calculated with using obtained in previous steps data:

$$C_P = \frac{P}{P_{wind}} = \frac{8}{\lambda^2} \int_{\lambda_h}^{\lambda} Q\lambda_r^3 a'(1-a)\left[1 - \frac{C_D}{C_L}tan\beta\right]d\lambda_r \tag{8.4.1}$$

With the use of trapezoids rule this integral can be transformed into the next one according to (Ingram G. 2005):

$$\int_{x_0}^{x_n} f(x)dx \approx \frac{x_n - x_0}{2n}[(y_0 + y_n) + 2(y_1 + y_2 + \cdots + y_{n-1})] \tag{8.4.2}$$

In our case $n = 1, x$ is replaced by λ_r, the function $f(x) = Q\lambda_r^3 a'(1-a)\left[1 - \frac{C_D}{C_L}\tan\beta\right]$. This equation is applied for to each blade section, so the sum gives the total power coefficient.

The described methodology does not take into account the change in lift and drug coefficients depending on the Reynolds number. It is assumed that calculated parameters change depends only on the relative angle of attack. This lack can be eliminated if the experimental curves will contain the dependence on the Reynolds number.

As a result of iteration process power coefficients were calculated for wind blade with and without ice. Also power coefficient as a function of tip speed ratio was estimated. Figure 8.4.1 shows these functions for clean and iced blade.

As can be seen from Figure 8.4.1 clean blade power efficiency is higher than iced blade. In order to keep wind turbine blade performance with the power coefficient highest value optimal angle of attack should be followed. Along with wind direction change blade pitch angle changes, so the angle of attack takes optimal value. In order to control power performance of the turbine characteristics with different pitch angles should be calculated. Described above algorithm allows to calculate the power coefficient value with various blade pitch angles and tip speed ratios. Figure 8.4.2 shows such dependence for clean blade.
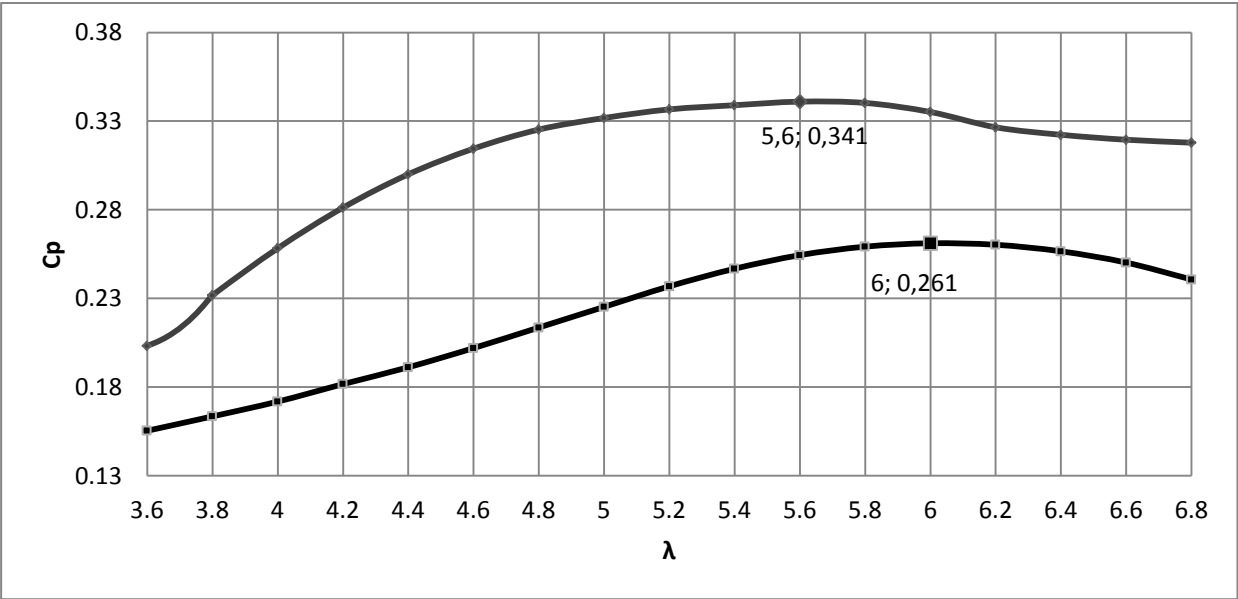

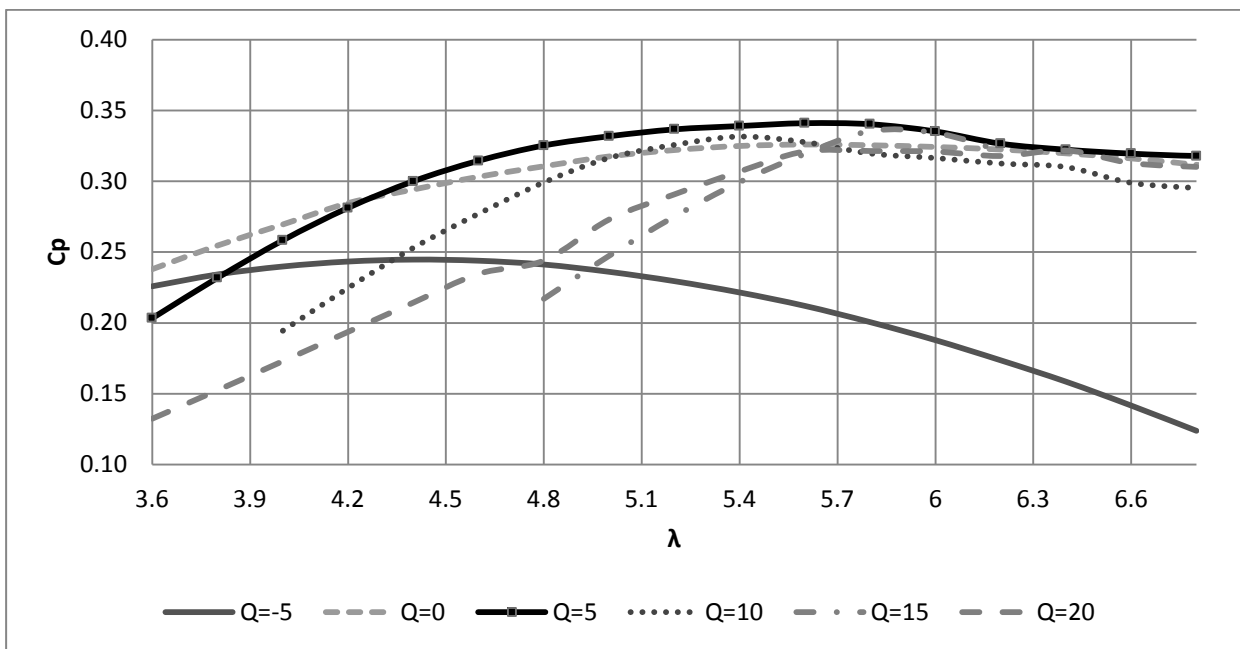Figure 8.4.1 Power coefficient vs tip speed ratio dependence.

Figure 8.4.2 Power coefficient Cp vs tip speed ratio for various blade pitch angle. Clean blade.

As can be seen from Figure 8.4.2 when blade pitch angle is $Q = 5°$ blade efficiency is higher. For the further calculation linear function between $\lambda = 0$ and $\lambda = 3,6$ is assumed. Maximum value of tip speed ratio is limited by resulting angle of attack and hence induction factor value.

8.5 Power curve prediction

Wind turbine power curve prediction involves consideration of the rotor, generator and control system. It can be divided into 3 areas according to wind velocity value: area before start-up speed, working area before nominal power achievement, area after nominal power achievement till the maximum allowable wind speed. The power curve in the second area can be calculated from matching the power output from the rotor as a function of wind speed and rotational speed to the power produced by the generator. (Manwell J.F., McGowan J.G. et al. 2009) Potential performance field is obtained for the number of rotor speeds and hence blade tip speed ratio:

$$n_{rotor} = \frac{30}{\pi} \lambda \frac{V}{R} \qquad (8.5.1)$$

$$P_{rotor} = C_P \eta \frac{1}{2} \rho \pi R^2 V^3 \qquad (8.5.2)$$

In the equation 8.5.2 power coefficient C_P is taken according to tip speed ratio λ and pitch angle $\theta = 0$. The next step is generator choosing. According to the blade radius 100 kW was chosen as generator power. Presented search considers synchronous

generators with 1500 revolution per minute and two different gearbox values: 22:1, 34:1. The points when rotor power is equal to the generator power are power curve points. Two generators were chosen in order to demonstrate two power curves with different wind velocity provided nominal rotor power.
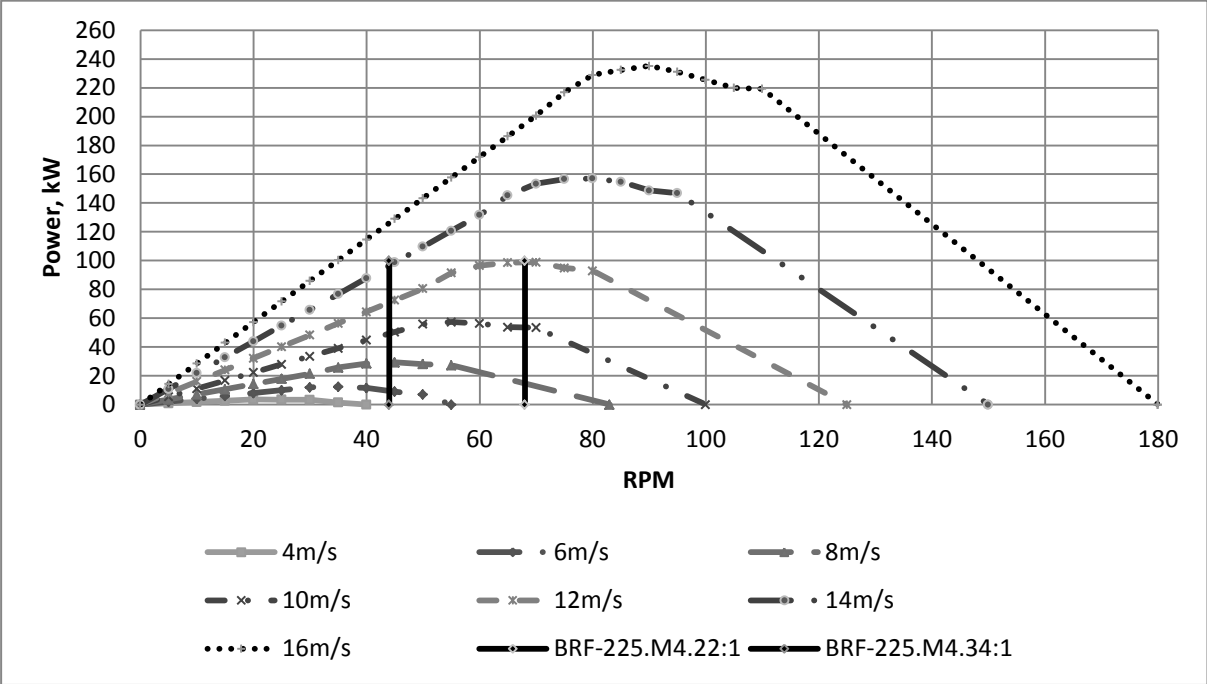

Figure 8.5.1 Rotor and generator power vs rotor speed with various wind speed. Clean blade.

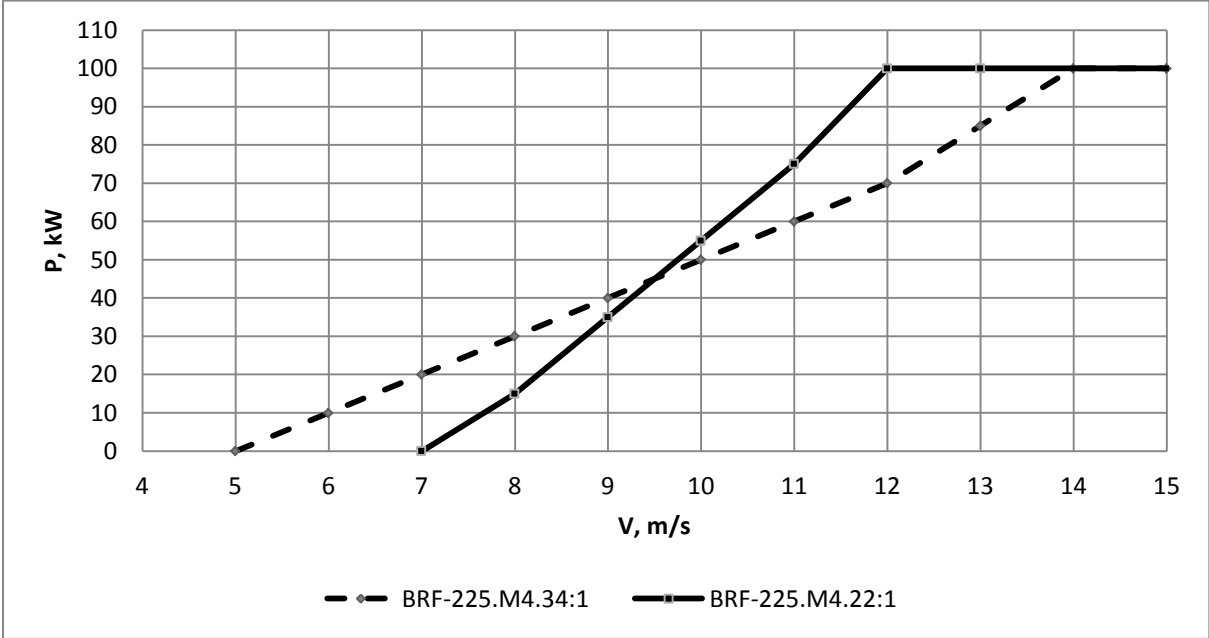Figure 8.5.1 data analyses gives three generators power curves.

Figure 8.5.2 Power curves families. Clean blade.

Generator BRF-225.M4 (100kW) characteristics can be found on the official webpage of "LitEnergo" company: (LitEnergo).

According to the wind velocities probability in considered region different types of generators should be investigated.

The same calculations were made with the iced wind blade. The power curve characteristics are presented on the Figure 8.5.3.
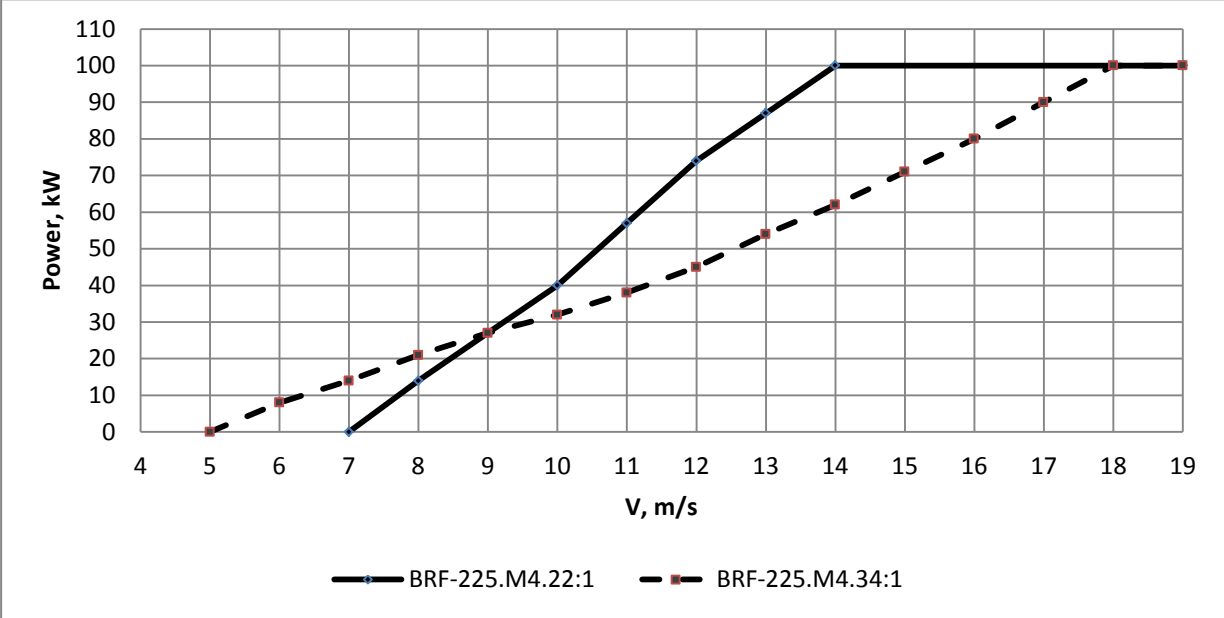

Figure 8.5.3 Power curves families. Blade with ice accreted.

In order to compare obtained results clean blade and iced blade characteristics are presented on the Figure 8.5.4.

As can be seen on the Figure 8.5.4 iced blade turbine can be characterized like almost new one. Nominal power wind speed is higher in case of BRF-225.M4.22:1 generator using in iced conditions. When using BRF-225.M4.34:1 nominal generator power can be obtained with wind speed 18 m/s. Presented calculations were made with 44% of ice load with ice shape A type according to (Seifert H. 1997) data. It is interesting to mention, that described blade with specified profile performance is even impossible with ice load level up to 22% with ice shape B type.
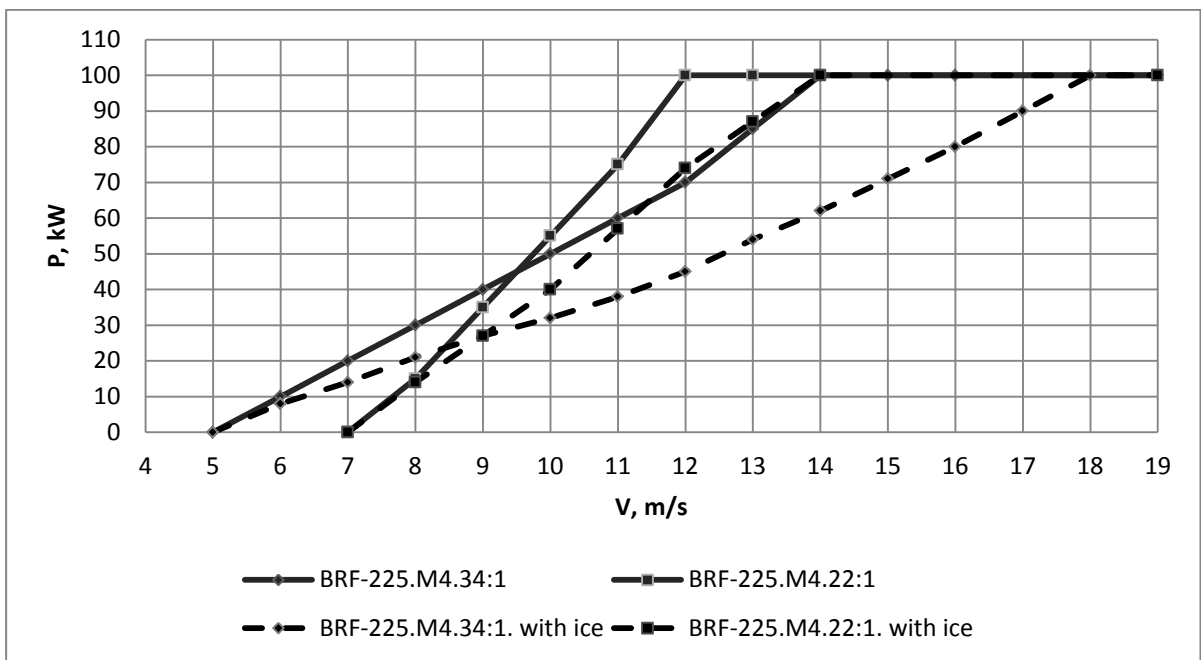
Figure 8.5.4 Power curves comparison.

9. Economic estimation of the ice accretion influence

Figure 8.5.4 shows that ice accretion decreases wind turbine efficiency. In order to illustrate ice influence blade with and without antyicing heating energy system were compared.

9.1 Geographical place description

Thesis considers wind turbine installed in the Lapland region (Sodankyla and Pallas). Meteorological data were taken from Finnish Meteorological Institute official website. (The Finnish Meteorological Institute) As an input meteorological data relative humidity, air temperature and wind speed measurements every 10 min during 2008 year were considered. According to (Homola M. C. 2005) the next list of meteorological factors should be met for ice accretion on the blade: relative humidity$>85\%$, air temperature$<0℃$. Calculated power curves do not depend on the kind of accreted ice. That is why ice accretion conditions are so general. The hub height is 100m.

9.2 Produced energy calculation

Two turbine performance modes are considered. The first one suggests heating system. In case if according to selected parameters value ice is accreted on the blade

5% of the nominal power is lost on the heating system. During the rest time without ice wind blade produces energy without losses. In the second mode in case of ice accretion wind turbine continue to work with ice on the blades. Calculation assumptions:

1) work does not consider time spent on ice melting;

2) wind turbine works without consumer load influence. All produced energy is consumed by system;

3) calculation does not consider turbine own needs, the aim is to illustrate ice influence and heating system payback;

4) work does not consider runback water path and influence;

5) work does not consider accreted ice shape and load calculation. Blade ability to work with accreted ice is not calculated. Maintenance price when working under conditions is not taken into account.

According to the described conditions produced energy with heating system, which goes out from the generator further in the net, is $83\,590$ kWh and without heating system $69\,489$ kWh. It accords to $16,9\%$ energy losses. If the price of 1 kWh of energy is suggested as $0,12$ € the heating system implementation can bring approximately 1692€ in specified place and described conditions.

According to suggested conditions turbine works $44,8\%$ of the total time per year. Annually $6\,545$kWh energy is spending on the heating system. If compare to the total produced energy in the mode with heating system it is equal to $7,8\%$ of the total produced energy. In order to decrease this share experiments on the site should be made. The required energy for the heating system should be determined according to the site conditions. Blade temperature sensors should be installed in order to escape blade overheating. In addition black paint can be used to heat blade naturally. In that case the required energy for the heating system also should be recalculated.

10. Conclusions

Since in the recent time problem of energy sources lack becomes more critical the renewable sources of energy utilization is one of the problem solutions. Among this kind of energy source wind energy is the most promising area. With the wind energy development more earth areas are being used with different environment conditions

and energy demand. According to blade technology climate conditions have to be taken into account when planning wind turbine operation. Nowadays sites with cold climate conditions became more attractive for wind energy utilization. That is why wind turbine design stages should be considered with respect to ice accretion influence.

Among the ice accretion influence not only energy losses can be mentioned, but operation reliability, public safety, maintenance management and turbine control. In this regard, for the analyses purposes wind turbine blades were chosen. Considering the aerodynamic parameters associated with the energy production and blade operation, ice accretion influence was tried to estimate and determine.

Aerodynamic parameters were determined used classical theory of moments. The blade was divided into sections and each section parameters were calculated. The total characteristic was obtained by integration all sections. Lift and drag coefficients are considered dependent only on the angle of attack, but not wind speed. Also some maintenance operation problems were not taken into account because of the lack of such information when operating in cold climate conditions. In addition one of the biggest problem with which wind energy engineer can face is the lack of lift and drag coefficients data, obtained from tunnel experiments with ice accreted on the blade. These characteristics have strong influence on the blade operation process and produced energy. That is why in addition to already existed lift and drag characteristics of clear blade profile new one with ice accreted on the blade should be investigated.

For the analysis of the ice accretion influence the test wind turbine of the Danish National Institute RISO was chosen. The blade radius is 9,5m and the tower height is 100 m. According to wind tunnel experiments made in Germany lift and drag coefficients of the iced blade were obtained. The wind turbine profile under investigation is NASA 4415. Among the available ice load the most light one was chosen, because with the other ice loads chosen blade is not able to operate. For the energy losses calculation the considered wind turbine location is Lapland region in Finland (Sodankyla and Pallas). Necessary weather conditions (wind speed, relative humidity, air temperature every 10 minutes during one year) was taken from The Finnish Meteorological Institute official database.

As results of calculations power coefficients were fond equal to $C_P = 0,261$ for the blade with ice accreted and $C_P = 0,341$ for the clean blade. For the clean blade pitch angle $Q = 5°$ appears to be more efficient. Synchronous 100 kW generators with different rotation speed were considered. The rotation speed was chosen in such a way that resulted power curve can match different wind source sites utilization. Obtained power curves show that wind blade with ice accreted behaves like almost new blade with the new characteristics. Furthermore produced energy by the two wind turbines installed in Lapland region was calculated. It is assumed that in one case heating system is installed and consumes 5% of produced by wind turbine energy. In the other case wind turbine operate without heating system and all accreted ice can be melted naturally or continue to move on the turbine. With the operation and meteorological assumptions the produced energy losses are equal to $16,9\%$. Turbine works $44,8\%$ of the total year time. Energy losses for the heating system is equal to $7,8\%$ of the total produced energy. Evidently each site will have its own characteristics of ice accretion and hence energy losses. Nevertheless in particular site with specified assumptions heating system appears to be the solution of ice accretion problem. The required energy for the heating system can vary according to specified site climate conditions. Generally difference in power coefficient value shows that ice accretion on the blade decreases wind turbine performance efficiency.

In order to eliminate or at least decrease ice accretion influence on the wind turbine operation more reliable and full data should be measured in the cold climate sites. Lift and drag coefficients of the blade profiles with the ice accreted should be experimentally obtained. It is interesting to modify wind blade profile in such a way, that ice accretion would be difficult and hence the more share of time wind turbine can operate with the clean blade and higher efficiency. In order to achieve this gain ice accretion on the different shape objects should be investigated. All these tasks are the challenge for the following research and development, which should be applied in wind energy technology and science.

References

(Krenn A. 2011a)   Krenn A., Windfarm Moschkogel in the Austrian Alps, 2011.

(Krenn A. 2011b)   Krenn A., The Alps – Windy, but also icy, 2011, Winterwind 2011.

(Makkonen L.(Ed.) 1994)   Makkonen L.(Ed.), 1994. Ice and construction. Rilen Report 13. London: E. & FN Spon.

(Böhmeke G. 1992)   Böhmeke G., 1992. Wind power plants in the weather conditions of Northern Finland. Valtion teknillinen tutkimuskeskus, Espoo.

(Morgan C., Bossanyi E. 1998)   Morgan C., Bossanyi E., Seifert H., 1998. Assessment of safety risk arising from wind turbine icing. Boreas IV.

(Ronsten G. 2008)   Ronsten G., 2008. Summary of a cold climate wind energy conference (2005).

(Ronsten G., Dierer S. 2009)   Ronsten G., Dierer S., Egil B., Nygaard K., Makkonen L., Homola M., 2009. Measures needed for the successful development of the wind energy in icing climates.

(Gedda H. 2011)   Gedda H., 2011. State of the art and benefit of de-icing and anti icing technologies for wind turbine operating in areas with icing condition.

(Seifert H. 1997)   Seifert H., 1997. Aerodynamics of iced aerfoils and their influence on loads and power production.

(Ingram G. 2005)   Ingram G., 2005. Wind turbine blade analysis using the blade element momentum method. Version 1.0. School of engineering, Duhram University.

(Beurskens J. 2011)   Beurskens J., 2011. A European perspective of wind energy in cold climates.

(Schepers J.G., Brand A.J. 2002)   Schepers J.G., Brand A.J., Bruining A., Graham J.M.R., Hand M.M., Infield D.G., Madsen H.A., Maeda T., Paynter J.H., R. van Rooij, Shimizu J., Simms D.A., Stefanatos N., 2002. Final report of IEA AnnexXVIII: 'Enhanced Field Rotor Aerodynamics Database'. ECN-C--02-016.

(Makkonen L., Laakso T. 2001)   Makkonen L., Laakso T., Marjaniemi M., Finstad K.J., 2001. Modelling and prevention of ice accretion on wind turbines. Wind Engineering, **25**(1), pp. 3-21.

(LitEnergo)   LitEnergo, http://www.litenergo.ru/PRO/production414.

(Homola M. C. 2005)   Homola M.C., 2005. Impacts and Causes of Icing on Wind Turbines. Narvik University College.

(Homola M. C., Nicklasson P. J. 2006)   Honmola M.C., Nicklasson P.J., Sundsbo P.A., 2006. Ice sensors for wind turbines. Cold Regions Science and Technology, **46**, pp. 125-131.

(Makkonen L. 1998)   Makkonen L., 1998. Modeling power line icing in freezing precipitation. Atmospheric Research, **46**(1-2), pp. 131-142.

(Makkonen L., Ahti K. 1995)   Makkonen L., Ahti K., 1995. Climatic mapping of ice loads based on airport weather observations. Atmospheric Research, **36**(3-4), pp. 185-193.

(Manwell J.F., Mcgowan J.G. 2009)   Manwell J.F., Mcgowan J.G., Rogers A.L., 2009. Wind energy explained. Theory, Design and Application. Second edition. Wiley.

(Moriarty P. J., Hansen A. C. 2005)   Moriarty P. J., Hansen A. C., 2005. AeroDyn Theory Manual. NREL/TP-500-36881.

(Parent O., Ilinca A. 2011)   Parent O., Ilinca A., 2011. Anti-icing and de-icing techniques for wind turbines: Critical review. Cold Regions Science and Technology, **65**(1), pp. 88-96.

(Cattin R. 2011)   Cattin R., 2011. Wind turbine blade heating – does it pay?

(Westerlund R. 2011)   Westerlund R., 2011. To De Ice or Not To De Ice. Measured power losses in wind power plants due to icing.

(Sell S. 2011)   Sell S., 2011. Anti-icing: surfaces, technical approaches and status, Fraunhofer IFAM.

(Laakso T., Holttinen H. 2003)   Laakso T., Holttinen H., Ronsten G., Tallhaug L., Horbaty R., Baring-Gould I., Lacroix A., Peltola E., Tammelin B., 2003. State-of-the-art of wind energy in cold climates. IEA R&D Wind.

(Laakso T., Tallhaug L. 2011)   Laakso T., Tallhaug L., Ronsten G., Cattin R., Baring-Gould I., Lacroix A., Peltola E., Wallenius T., Durstewitz M., Hullkonen M., Krenn A., 2011. Wind energy in cold climates IEA task 19.

(The Finnish Meteorological Institute)   Kukkurainen N. 2010.The Finnish Meteorological Institute. Available at: http://en.ilmatieteenlaitos.fi/home..

(Carlsson V. 2011)   Carlsson V., 2011. Measuring routines of ice accretion for wind turbine applications. The correlation between production losses and detection of ice.

(Wright W.B., Rutkowski A. 1999)   Wright W.B., Rutkowski A., 1999. Validation Results for LEWICE 2.0. National Aeronautics and Space Administration Lewis Research Center.

(Wright W.B. 2002)   Wright W.B., 2002. User Manual for the NASA Glenn Ice Accretion Code LEWICE version 2.2.2. National Aeronautics and Space Administration.
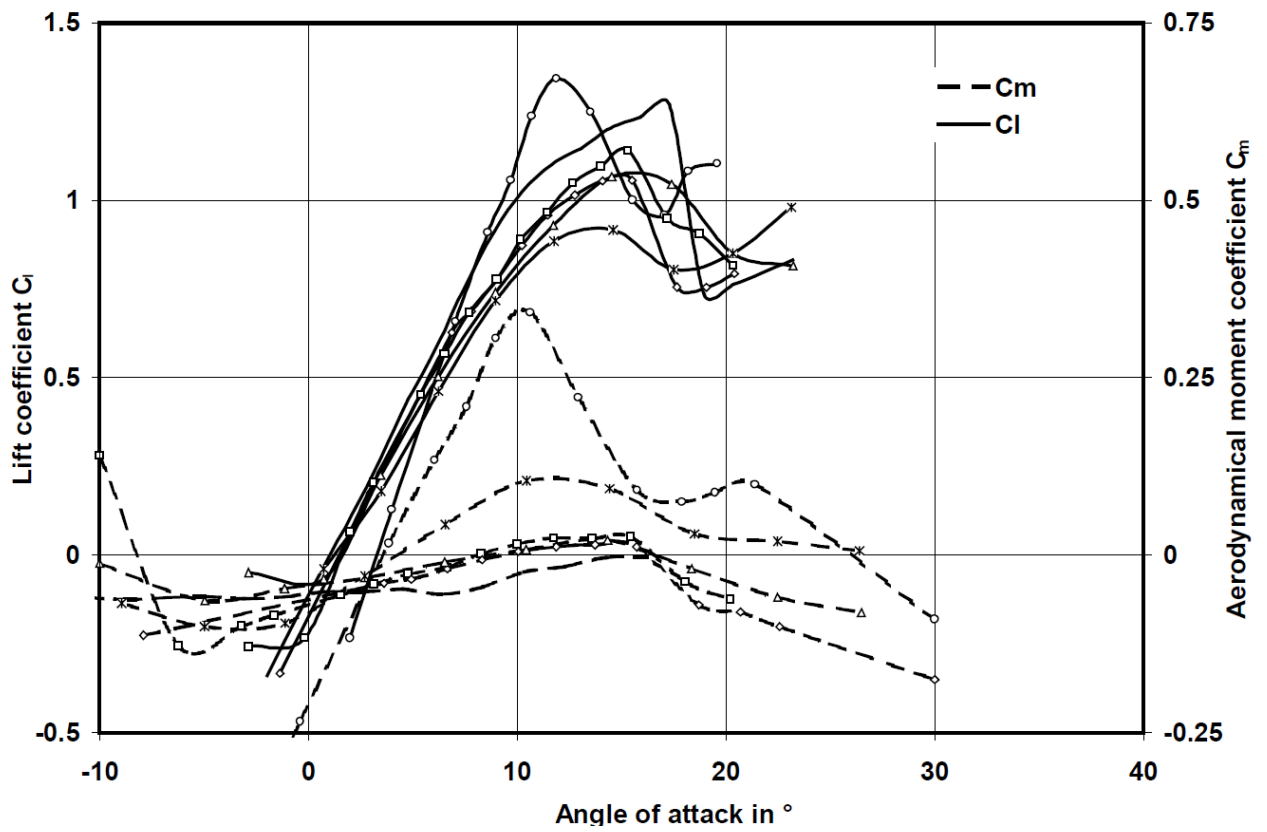
Appendix 1. Experimental data
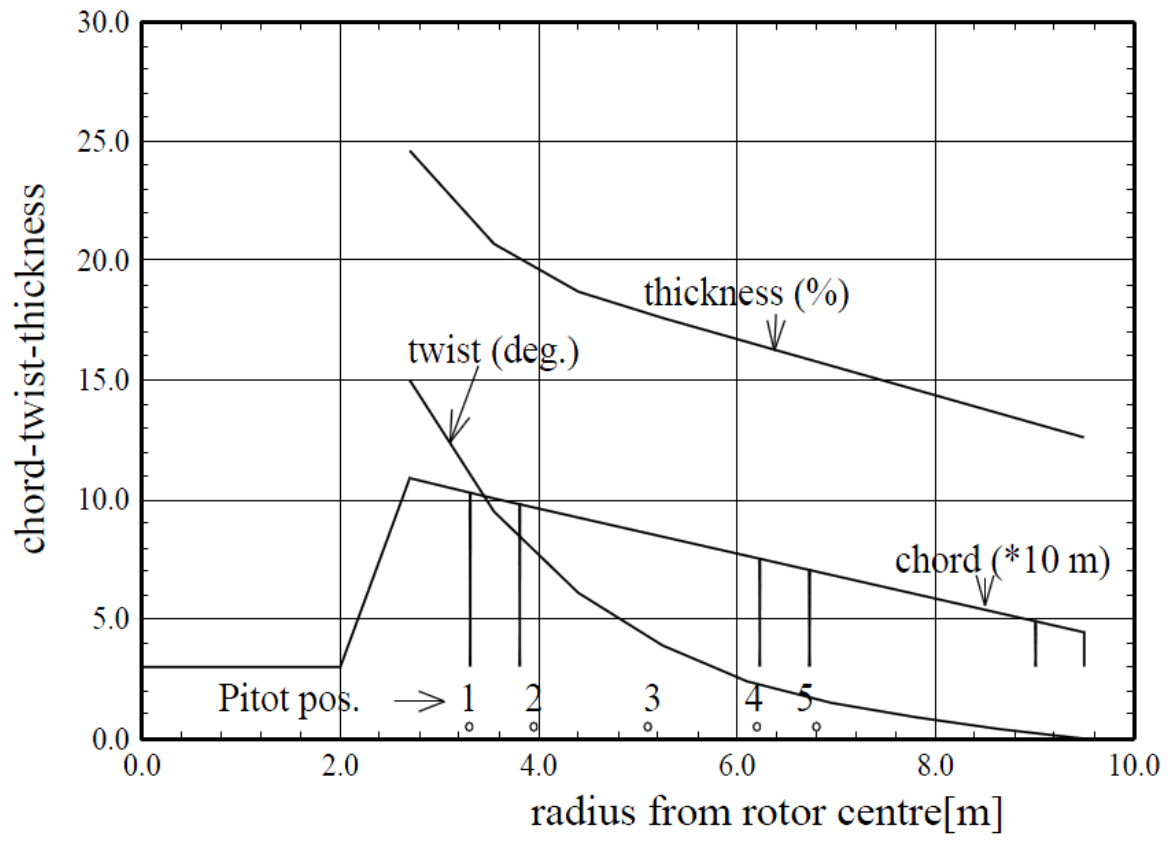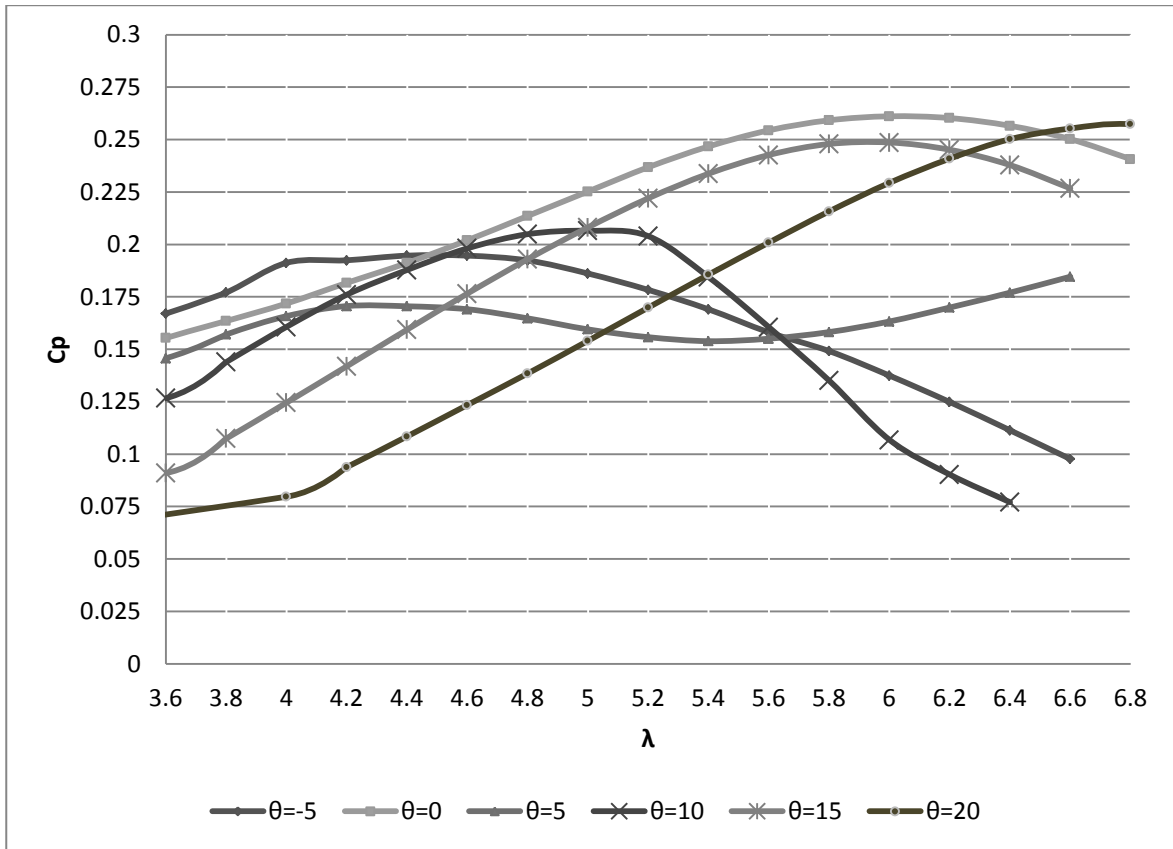

RISO test turbine characteristics.
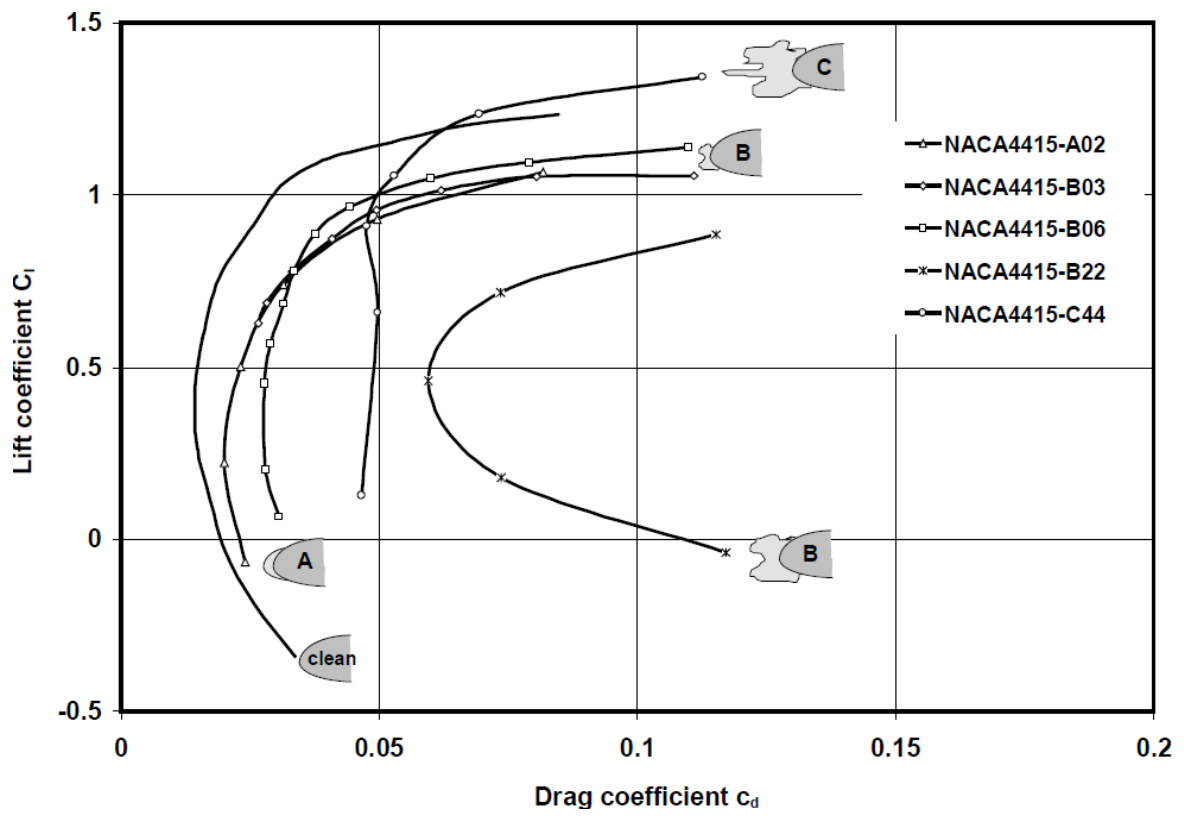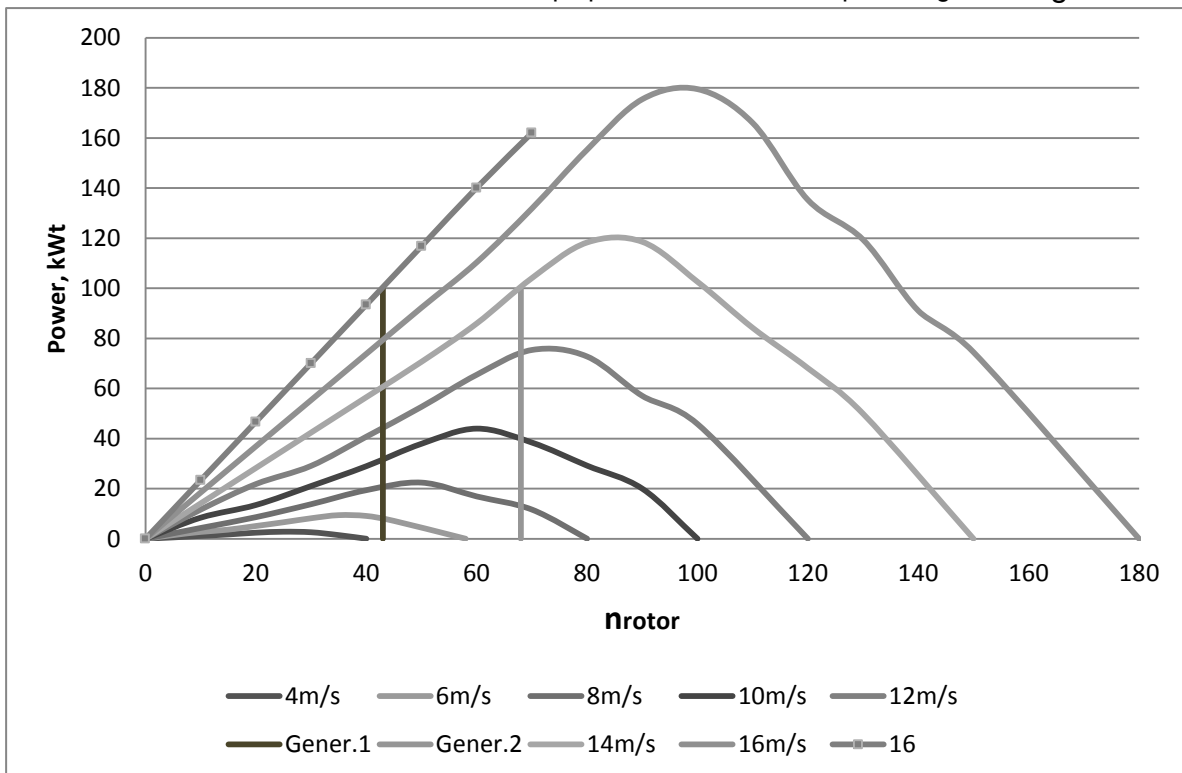
Lift and drag coefficients dependence.

Lift coefficient vs angle of attack dependence.

Blade with ice. Power coefficients function vs tip speed ratio with blade pitch angle change.

Blade with ice. Turbine power function vs rotation frequency.